

A Review on CeO₂-Based Electrocatalyst and Photocatalyst in Energy Conversion

Qingqing Li, Lianpeng Song, Zhong Liang, Mingzi Sun, Tong Wu, Bolong Huang,*
Feng Luo, Yaping Du,* and Chun-Hua Yan

The activation and conversion of small molecules (H₂, O₂, H₂O, CO₂, N₂, CH₃OH, and C₂H₅OH) in energy-related systems has attracted researchers' attentions around the world. The conversion of these molecules plays a key role in renewable energy storage and conversion systems, and for that, the electrocatalysis and photocatalysis processes are considered as clean and efficient strategies. Numerous materials are designed to promote the conversion process to satisfy the different requirements for efficiency and selectivity. Due to the flexible switching between Ce³⁺ and Ce⁴⁺ with rich oxygen defects, CeO₂-based materials display excellent performance in all the related reaction processes. Herein, the CeO₂-based electro(photo)catalysts according to different reactions are summarized. Specifically, the influence of material compositions, morphologies, and structures on catalytic performance is discussed, and the significant role of CeO₂ is emphasized. Finally, several approaches are advocated to promote the development of CeO₂-based electro(photo)catalysis and accelerate their industrial application.


dioxide relieves the greenhouse effect and provides the chemical feedstocks through a carbon recycle (carbon monoxide, formate, formaldehyde, methane, methanol, and C₂₊ hydrocarbons and oxygenates).^[3] Water splitting, which comprises two half-cell reactions, can provide us with clean hydrogen as fuel.^[4] Fuel cell is a type of environmental friendly energy-conversion device with two half-reactions as oxygen reaction and fuel oxidation.^[5] In addition, nitrogen reduction reaction can convert the dinitrogen molecules in the atmosphere into ammonia, a higher-value product.^[6] To cleanly and sustainably realize the activation and efficient conversion of the above energy molecules, one prospective goal is to develop electrochemical and photochemical process. The key to enable this vision is the development of improved electrocatalysts and photocata-

1. Introduction

With the increasing energy demands and the impending climate change, the researchers have to turn their attention to develop sustainable and clean pathways to produce fuels and chemicals. Creating a global-scale sustainable energy system for the future to preserve our environment is one of the most crucial challenges facing humanity today.^[1] High-efficiency conversion of electrical energy from renewable energy sources (such as wind energy, solar energy, etc.) into chemical energy is an effective strategy for making full use of and storing energy.^[2] Reducing carbon

lysts with high efficiency and selectivity for the energy molecules transformations involved.^[2] A number of catalysts have been developed for the related reaction such as hydrogen evolution reaction (HER),^[7] hydrogen oxidation reaction,^[8] oxygen evolution reaction (OER),^[8] oxygen reduction reaction (ORR),^[9] methanol/ethanol oxidation reaction (M/EOR),^[10] carbon dioxide reduction reaction (CO₂RR), and nitrogen reduction reaction (NRR).^[11] Currently, the IrO₂, RuO₂, and Pt/C are the benchmarking electrocatalysts for these catalytic processes; however, the scarcity and high cost of these materials limit its wide applications. Although various metal-based, metal oxide-based, and

Q. Li, L. Song, Z. Liang, Prof. F. Luo, Prof. Y. Du, Prof. C.-H. Yan
Tianjin Key Lab for Rare Earth Materials and Applications
Center for Rare Earth and Inorganic Functional Materials
School of Materials Science and Engineering
National Institute for Advanced Materials
Nankai University
Tianjin 300350, China
E-mail: ypdu@nankai.edu.cn

 The ORCID identification number(s) for the author(s) of this article can be found under <https://doi.org/10.1002/aesr.202000063>.

© 2021 The Authors. Advanced Energy and Sustainability Research published by Wiley-VCH GmbH. This is an open access article under the terms of the Creative Commons Attribution License, which permits use, distribution and reproduction in any medium, provided the original work is properly cited.

DOI: 10.1002/aesr.202000063

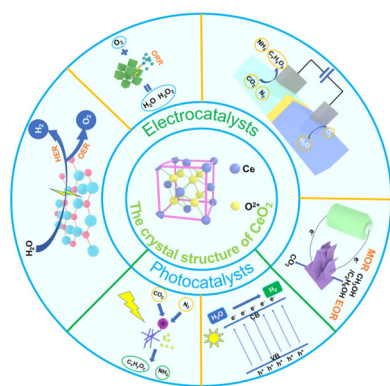
M. Sun, T. Wu, Prof. B. Huang
Department of Applied Biology and Chemical Technology
The Hong Kong Polytechnic University
Hung Hom, Kowloon, Hong Kong SAR, China
E-mail: bhuang@polyu.edu.hk

Prof. C.-H. Yan
Beijing National Laboratory for Molecular Sciences
State Key Laboratory of Rare Earth Materials Chemistry and Applications
PKU-HKU Joint Laboratory in Rare Earth Materials and Bioinorganic Chemistry
College of Chemistry and Molecular Engineering
Peking University
Beijing, China

Prof. C.-H. Yan
College of Chemistry and Chemical Engineering
Lanzhou University
Lanzhou 730000, China

carbon-based catalysts have been extensively studied, there is still room for further improvement in their activity, stability, and cost. A number of photocatalysts also have been designed and researched; however, the conversion efficiency of light to chemical energy and the selectivity for targeted products are far from satisfactory hitherto. It is worth noting that, in the development of high-efficient electrocatalysts and photocatalysts, CeO₂ plays an important role in enhancing the catalytic performance due to its unique physical and chemical properties.^[12–15]

CeO₂, a rare earth oxide widely studied, has shined in thermocatalysis, electrocatalysis, and photocatalysis (Scheme 1). CeO₂ nanocrystal has the fluorite crystal structure with space group *Fm3m* and the cell parameters of 0.5411 nm (*a* = *b* = *c*). In the CeO₂ unit cell, each Ce⁴⁺ is coordinated with eight adjacent O²⁻ to form an octahedral interstitial, and each O²⁻ is coordinated with four adjacent Ce⁴⁺ to form a tetrahedral unit.^[16] The unfilled 4f orbital and abundant electronic energy levels endow CeO₂ to have a great potential in catalysis. The electronic structure of Ce is [Xe] 4f¹5d¹6s², where Ce³⁺ and Ce⁴⁺ are able to exist steadily and convert to each other easily. The multivalence property of CeO₂ will offer the opportunity to generate strong interactions with other components in catalysts and thereby enhance the performance of electrocatalysts and photocatalysts.^[17] In addition, the unique crystal structure and reversible valence characteristics of CeO₂ enable the formation of oxygen vacancies to generate a defect-rich structure, which determines the excellent catalytic performance. Oxygen vacancy, derived from Ce⁴⁺ to Ce³⁺ reduction conversion or lattice oxygen migration, has a great influence on the electronic and chemical properties of CeO₂. In the catalysts, oxygen vacancy not only anchors active component nanoparticles or clusters but also regulates the electronic structure of catalysts.^[18] It also has impact on the bandgap, light-harvesting, and electron–hole pair recombination of catalysts, which closely related to photocatalytic activity. Moreover, the high stability of CeO₂ in both acidic and alkaline environments is also favored to electrocatalytic process. Based on the unique physical and chemical properties of CeO₂, tuning the size, structure, and exposed crystal planes is a promising strategy to construct the high-efficient CeO₂-based electrocatalysts and photocatalysts. This field is developing rapidly and a timely review on both electrocatalysts and photocatalysts in energy conversion is great of meaningful.



Scheme 1. Illustration of CeO₂-based electro(photo)catalysts in energy-related small molecules conversion.

2. CeO₂-Based Electrocatalyst

2.1. Hydrogen Evolution Reaction

In response to the rapid depletion of fossil fuel and growing environmental problem issues, researchers have turned their attention to the clean molecular hydrogen energy, which is usually generated by the water splitting effectively and conveniently. As a half reaction of water splitting, HER is a two-electron transfer reaction and generally involves the Volmer–Tafel path or the Volmer–Heyrovsky path. To achieve large-scale industrial hydrogen production, highly active catalysts are required to lower the overpotential for HER. Due to the strong electronic interactions, CeO₂ usually has a strong electronic interaction with other materials and then regulate their electronic structure, so it often is chosen to be support or other key component to fabricate HER catalysts. Due to the poor conductivity of CeO₂, the strategy of compositing CeO₂ with highly conductive materials is often used to enhance the activity of CeO₂-based electrocatalysts.

Liu et al. constructed 3D reduced graphene supported CeO₂ hollow microspheres by a hydrothermal self-assembly method to catalyze HER.^[19] Enhanced activities with low onset overpotential of 192 mV and overpotential of 340 mV at a current density of 10 mA cm⁻² are achieved due to the highly conductive network and rich porous structure on 3D reduced graphene. Novel metal catalysts usually have high catalytic activity, and the activity will be improved if combined with a suitable support. Gao et al. fabricated sub-nanometer Pd clusters confined in porous CeO₂ and the electrochemical results of the obtained catalysts show nearly 100 times higher activity HER than Pt/C catalyst at low-potential region.^[20] The adsorption state of H* on the Pd cluster is effectively modulated by the electron transfer between Pd and O atoms, and then, the conjoint effect promotes the HER catalytic activity.

Another work by Gao et al. reached similar conclusions, where the electron transfer from Pd to CeO₂ leads to oxidized Pd and formation of Pd–O–Ce structure, which provides a new catalytic active site for HER.^[21] Rh⁰/CeO₂ and Ru⁰/CeO₂ catalysts were also prepared for HER, which both have exceptional durability in an acidic environment for over 10 000 scans.^[22,23] These results indicated that CeO₂ not only plays as an activity enhancer but also as a catalyst stabilizer. In addition to novel metal catalysts, nonprecious metal-based catalysts such as 3d transition metals Fe, Co, and Ni also have good catalytic performances for HER. The 3D porous Ni/CeO₂ nanosheet array supported on Ti mesh was prepared by Sun et al. to boosting HER for both high catalytic activity and good durability were achieved.^[24] Xiao et al. encapsulated different transition metals M (M = Fe, Co, and Ni) in carbon nanotubes and then supported with CeO₂ support (M@CNT/CeO₂) to compare the catalytic activity of Fe, Co, and Ni for HER.^[25] The results showed that the Co has a much higher activity for HER than Fe and Ni in M@CNT/CeO₂, which is consistent with density functional theory (DFT) calculation results. Most recently, Kang et al. prepared Co-doped CeO₂ nanosheets by a thermal decomposition exfoliation method. The introduction of Co atoms doped into CeO₂ crystal lattice generated more oxygen vacancies, which enable the fast water dissociation. As a result, the high surface, optimized hydrogen adsorption and

oxygen vacancies coordinatively contributed to the Co-doped CeO_2 as an efficient HER catalysts.^[26]

Transition metal phosphides have been studied for HER catalysts, and especially CoP has received the most attention. Xiong et al. fabricated nanohybrid CeO_2 -CoP-C catalyst by a co-ionic-exchange and low-temperature phosphorization method.^[27] The CeO_2 -CoP-C catalyst displayed an obvious enhancement in catalytic performance for HER compared to the CoP-C catalyst due to the synergistic reaction between CeO_2 and CoP. The synergistic reaction not only decreases the hydrogen absorption energy to promote gas escape but also optimizes the electronic structure of catalyst to more favorable for HER. In addition, a CoP/ CeO_2 interface was built to promote HER and DFT indicated that a lower water splitting energy barrier and more optimized hydrogen adsorption free energy are achieved compared to CoP by constructing CoP/ CeO_2 interface (Figure 1a-c).^[28] Similarly, the Ni_2P - CeO_2 interface was also fabricated and, as expected, has an enhanced HER activity (Figure 1d-f).^[29] Moreover, Ni_3N and Ni-S alloys, etc., were composited to CeO_2 and both generate good electrocatalytic properties

(Figure 1g-i).^[30-32] Therefore, the HER activity and stability of different catalysts including novel metal, transition metals, transition metal phosphides, and transition metal nitrides catalysts are enhanced by compositing CeO_2 since it tends to regulate and optimize the electronic structure of catalyst (Table 1). The optimized hydrogen adsorption free energy caused by adjusting the electronic structure of catalysts leads to a promoted HER performance.

2.2. Hydrogen Oxidation Reaction

Compared to proton exchange membrane fuel cells (PEMFCs), anion exchange membrane fuel cells (AEMFCs) catch more eyes due to the development of platinum group metal-free electrocatalysts. However, the sluggish kinetics of hydrogen oxidation reaction (HOR) in alkaline media and poor stability have impeded AEMFC development, so rational design and fabrication of highly active electrocatalysts to enhance HOR is of great significance. Bellini et al. construct Pd- CeO_2 /C to replace Pt

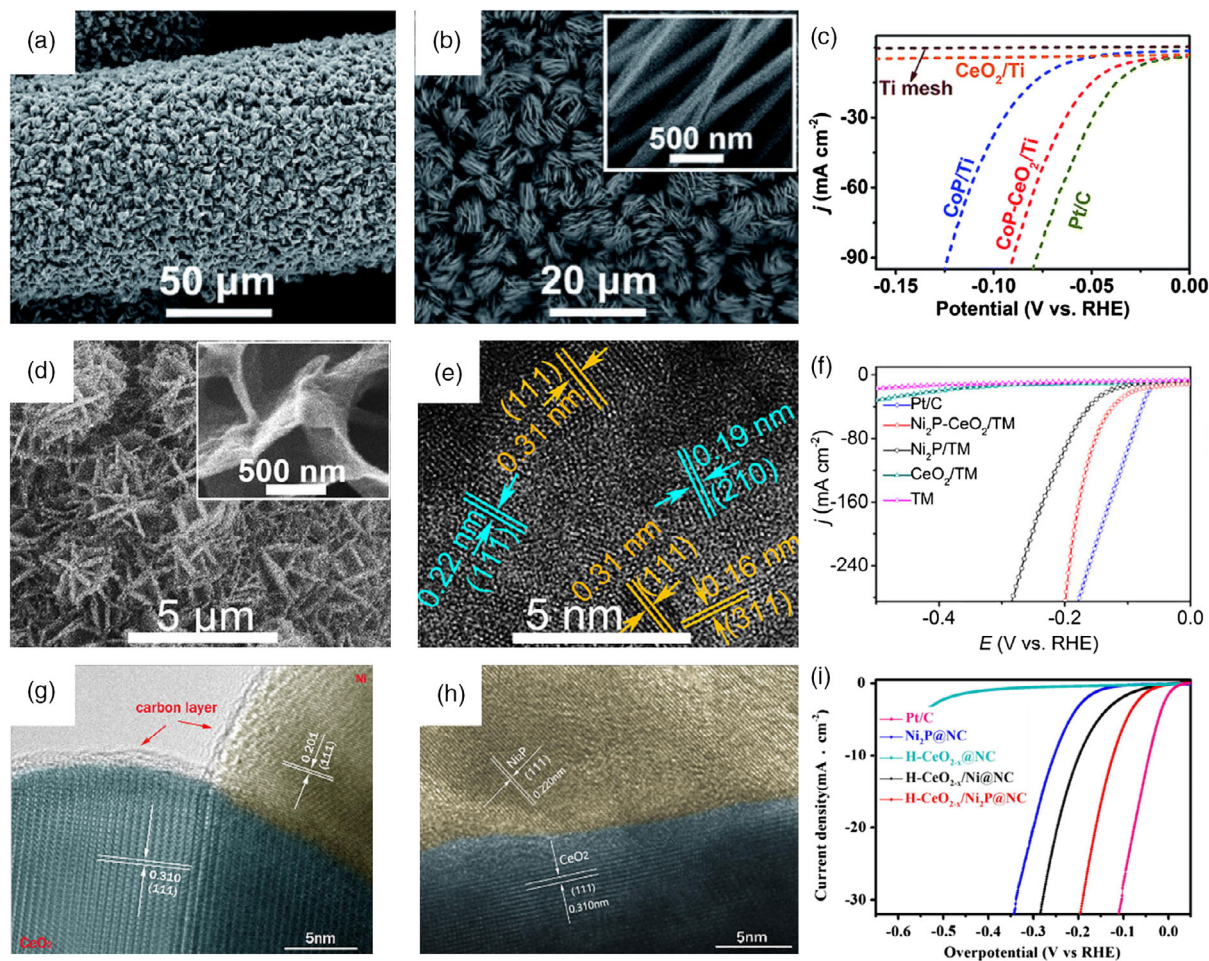


Figure 1. a,b) Scanning electron microscope (SEM) images of CoP- CeO_2 /Ti and c) polarization curves of Ti mesh, CeO_2 /Ti, CoP/Ti, CoP- CeO_2 /Ti, and Pt/C on Ti mesh for the HER at a scan rate of 2 mV s^{-1} Reproduced with permission.^[28] Copyright 2018, Royal Society of Chemistry. d,e) SEM and high-resolution transmission electron microscopy (HRTEM) images of Ni_2P - CeO_2 . f) Polarization curves for HER on Pt/C loaded on TM, Ni_2P - CeO_2 /TM, Ni_2P /TM, CeO_2 /TM, and bare TM. Reproduced with permission.^[29] Copyright 2018, American Chemical Society. g,h) HRTEM images of H- CeO_{2-x} /Ni@NC and H- CeO_{2-x} /Ni₂P@NC. (i) Polarization curves of different catalysts tested in 1.0 M KOH. Reproduced with permission.^[30] Copyright 2019, Elsevier.

Table 1. Summary of the HER catalytic property of various CeO₂-based electrocatalysts.

Electrocatalyst	Overpotential @10 mA cm ⁻² [mV]	Tafel slope [mV dec ⁻¹]	Electrolyte	Ref.
3D-rGO-CeO ₂	340	112.8	1 M KOH	[19]
Pd/CeO ₂ /C	109	75	1 M KOH	[21]
Ru ⁰ /CeO ₂	47	41	0.5 M H ₂ SO ₄	[22]
Rh ⁰ /CeO ₂	42	34	0.5 M H ₂ SO ₄	[23]
Ni-CeO ₂ /Ti mesh	67	111	1 M KOH	[24]
Co@CNT/CeO ₂	181	90	1 M KOH	[25]
CeO ₂ -CoP-C	71	53	0.5 M H ₂ SO ₄	[27]
CoP/CeO ₂	43	45	1 M KOH	[28]
Ni ₂ P/CeO ₂	84 [20 mA cm ⁻²]	113	1 M KOH	[29]
Ni-S/CeO ₂	180	158	1 M NaOH	[31]
CeO _{2-x} /Ni ₂ P@NC	123	60	1 M KOH	[30]
Ni ₃ N-CeO ₂	80	122	1 M KOH	[32]

catalysts for promoting HOR.^[33] A peak power density of 1.4 W cm⁻² was achieved due to the engineered Pd-to-CeO₂ interfacial contact. Furthermore, the DFT calculations suggest that the enhanced HOR activity is ascribed to a weakening of hydrogen binding energy through the interaction of Pd with the oxygen of CeO₂, which is facilitated by the structure of “oxidized Pd atom coordinated by four O atom on CeO₂.” Similarly, the Pd/CeO₂ or Pd-CeO₂/C catalysts that were constructed by interface engineering,^[34] surface doping,^[35] entrapping,^[36] depositing,^[37] and so on show promoted activity for HOR.^[38,39] Not only Pd-based electrocatalysts but also the oxygen-vacancy-rich CeO₂/Ni heterostructures were also synthesized to enhance HOR.^[8] The thermoneutral adsorption free energies of H* caused by the electron transfer between CeO₂ and Ni combined with promoted OH* by abundant oxygen vacancies lead to an excellent HOR performance (0.038 mA cm_{Ni}⁻² and 12.28 mA mg_{Ni}⁻¹). Furthermore, the Ir/CeO₂-C also displayed an enhanced activity due to the oxophilic effect caused by the higher oxygen storage-release capacity of CeO₂.^[40] To summarize, CeO₂ is able to modulate the coordination environment of active components or sites to be more suitable for adsorbing H* and OH*, and so promote HOR.

2.3. Oxygen Evolution Reaction

As the other half-reaction of water splitting, OER is a four-electron transfer reaction, which is considered as the major bottleneck for water splitting because of the sluggish kinetics. Obviously, the OER is the key step to govern the overall efficiency of water splitting so that developing the highly active catalysts for OER is significant to improve the efficiency of water spitting. The conventional adsorbate evolution mechanism for HER is widely accepted and OH⁻ adsorbs on the surface oxygen vacancy site at the beginning.^[41] Oxygen vacancy in the catalysts that has been reported can affect the surface charge distribution and further promote OER. Therefore, the CeO₂ in OER catalyst not only functions as a support but

also mediates the surface charge distribution and regulates the adsorption/ desorption energy of reactants, products, and intermediates. Yang et al. prepared two morphologies of CeO₂ (nanowires and nanospheres) by the hydrothermal method and compared their OER activities. As a result, the nanospheres possess a stronger catalytic ability than nanowires due to the higher oxygen vacancy concentration in CeO₂ nanosphere.^[42]

Considering the poor conductivity of CeO₂, the hybrid electrocatalyst has been synthesized with a combination of different materials. Recently, a CeO₂ decorated reduced graphene oxide was fabricated and it shows an enhanced HER activity, which results from the synergistic effect of oxygen vacancies on CeO₂ and electronic conductivity of reduced graphene oxide.^[43] RuO₂ is one of the most active catalysts for OER, and researchers identified that the enhanced activity and stability in an alkaline solution of Ru⁰/CeO₂ and RuO₂/CeO₂ catalysts was attributed to the highly oxidative oxygen species O₂²⁻/O⁻ formed in the oxygen vacancy of CeO₂.^[44,45] Transition metal-based catalysts are also reported as the low-cost and highly active catalyst solution for the OER, which have been widely studied as an alternative to replace the precious metal catalysts. CeO₂ decorated Ni(OH)₂ catalysts were fabricated and their catalytic performance for OER was studied (Figure 2a-e).^[46,47] As a result, the introduction of CeO₂ nanoparticles not only creates more active species of Ni^{3+/4+} but also accelerates the charge transfer efficiency, which significantly promotes the OER (Figure 2f,g). Wu et al. reported a Ni₃S₂-CeO₂ hybrid nanostructure by an electrodeposition method. The interfacial interaction between Ni₃S₂ and CeO₂ improves the electron transfer and enhances OER activity by increasing the binding strength of the reaction intermediates at the interface.^[48] The bimetal alloy and hydroxide were also composited with CeO₂ to enhance the OER activity.^[49-53] Chen et al. constructed Fe_xNi_y/CeO₂/NC catalyst and attributed its enhanced OER activity to the high oxygen-storage capacity of CeO₂, which enabled the immediate adsorption of the generated O₂ during OER process.^[51] Transition metal oxide was considered as an important type of OER catalyst due to the remarkable redox capability and mixed valences. Therefore, transition metal oxide was fabricated as a special structure compositing with CeO₂ to promote OER. Hollow Co₃O₄/CeO₂ heterostructures embedded in N-doped carbon nanofibers were prepared by the electrospinning technique. The synergistic effects between Co₃O₄ and CeO₂ benefit the OER (Figure 2h-j).^[43] More recently, Qiu et al. combined CeO₂ and Co₃O₄ by built-in pn heterojunction to promote OER.^[54] The strongly coupled pn heterojunction interface leads to a rapid interfacial charge transfer from CeO₂ to Co₃O₄ and the resulting high concentration of oxygen vacancies and Co²⁺ octahedral sites enhances the OER activity. FeCoO₄/CeO₂ interface and 3D self-supporting porous network NiCeO_x@NiFeO_x structure were also fabricated to enhance OER activity and the increased oxygen vacancy due to Ce³⁺/Ce⁴⁺ was proved to promote the intrinsic OER activity of catalysts.^[52,53] A quinary metal oxide Ni_{0.3}Fe_{0.07}Co_{0.2}Ce_{0.43}O_x was prepared by Haber et al. to promote OER.^[55] Subsequently, a similar (Ni-Fe-Co-Ce)O_x was prepared by Favaro et al. and studied under the operando conditions to expand the fundamental understanding of the active site. It turns out that the

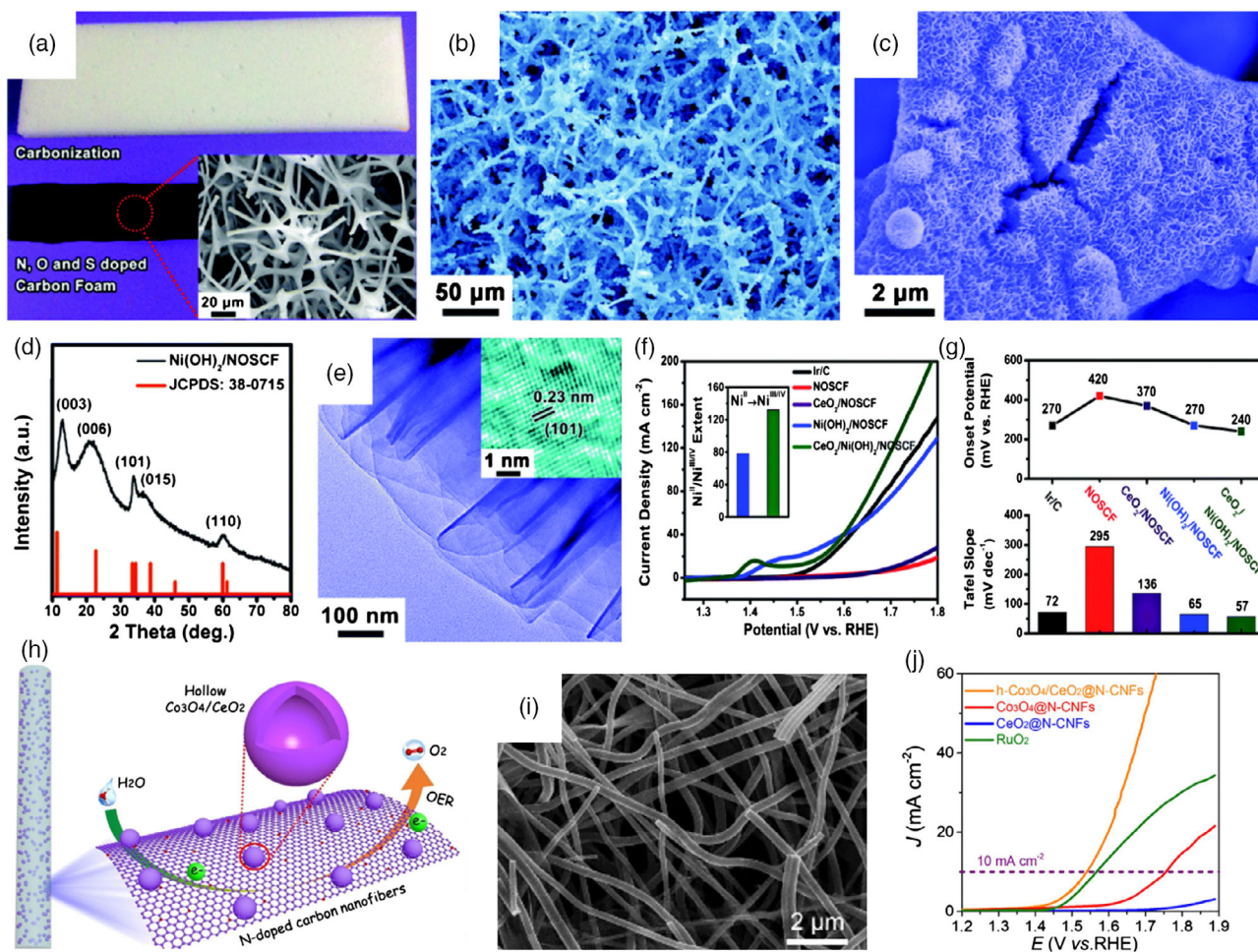


Figure 2. a) Carbon foam derived from a piece of melamine. b–d) SEM images and XRD pattern of Ni(OH)₂ nanosheets grown on NOSCF. e) HRTEM image of Ni(OH)₂ at the edge of the Ni(OH)₂/NOSCF. f) Polarization curves of different catalysts. g) The corresponding onset potential and Tafel curves for the catalysts derived from (f). Reproduced with permission.^[46] Copyright 2017, Royal Society of Chemistry. (h) Schematic diagram of hollow Co₃O₄/CeO₂ embedded in N-doped carbon nanofibers. i) SEM of h-Co₃O₄/CeO₂@N-CNFs. Reproduced with permission.^[43] 2019, American Chemical Society. j) Linear sweep voltammetry polarization curves of different catalysts in O₂-saturated 0.1 M KOH.

CeO₂ can affect the redox process of transition metals, which boosts the OER activity at low overpotential.^[56] Furthermore, several Co-based catalysts like Co, CoO_x, CoP, CoSe₂, and NiCo₂S₄ were combined with CeO₂ to enhance OER activity.^[57–61] CeO₂ not only enhances catalytic activity but also stabilizes the catalysts. Obata et al. coated CeO_x layer on NiFeO_x to prevent the loss of Fe species during the OER process and achieved a highly stable performance.^[62] The CeO_x layer does not affect the OER activity of NiFeO_x because it selectively allows the permeation of OH[−] and O₂ through but prevents the diffusion of redox ions through the layer. Conclusively, on the one hand, the oxygen vacancy on CeO₂ can promote the adsorption of OH[−], a step that occurs in OER. On the other hand, the oxygen vacancy often interacts with active components to produce special electronic structure that is conducive to the progress of OER, so, the rich oxygen vacancy in CeO₂ makes it a robust cocatalyst to enhance the catalytic activity of novel metal, transition metal, transition metal (hydro)oxides,

transition metal phosphides, and bimetal alloy for OER (Table 2).

Based on the attractive catalytic performance for HER and OER of CeO₂-based catalysts, the related materials were also designed for overall water splitting. Tang et al. prepared hollow CeO_x/CoP heterostructures supported on nickel foam through co-based metal-organic frameworks template. The potential toward water splitting at 10 mA cm^{−2} was only 1.63 V and the catalyst performed excellent stability within 60 h.^[63] Most recently, Du et al. synthesized superhydrophilic Co₄N–CeO₂ hybrid nanosheet array on a graphite plate for overall water splitting. The cell voltage to drive 10 mA cm^{−2} was 1.54 V and long-term durability at 500 mA cm^{−2} for 50 h. Doping CeO₂ into Co₄N not only promotes the dissociation of H₂O and adsorption of hydrogen but also improves the compositional stability, which boosting both OER and HER.^[64] Therefore, CeO₂-based materials have great potential for water splitting, and more reasonable components and structures need to be explored and designed.

Table 2. Summary of the OER catalytic property of various CeO₂-based electrocatalysts.

Electrocatalyst	Overpotential @ 10 mA [cm ⁻² mV]	Tafel slop [mV dec ⁻¹]	Electrolyte	Ref.
Ru ⁰ /CeO ₂	420	122.0	0.5 M KOH	[44]
Ni(OH) ₂ /CeO ₂	320 [100 mA cm ⁻²]	126.0	1 M KOH	[47]
3D CeO ₂ /Ni(OH) ₂ /C	–	57.0	1 M KOH	[46]
Fe _x Ni _y /CeO ₂ /NC	240	85.0	1 M KOH	[51]
Ni ₉₀ Fe ₁₀ /CeO ₂	369	70.7	1 M KOH	[50]
NiFe-LDH/CeO ₂ @CeNC	235	128.8	1 M KOH	[49]
Co ₃ O ₄ /CeO ₂	310	89.0	0.1 M KOH	[43]
NiCeO _x @NiFeO _x /Ni foam	254 [100 mA cm ⁻²]	59.9	1 M KOH	[52]
FeCo ₂ O ₄ /CeO ₂	–	63.0	0.1 M KOH	[53]
V-CoP@CeO ₂	225	58.0	1 M KOH	[57]
CeO ₂ /Co@NC	474	–	0.1 M KOH	[58]
CeO _x /CoO _x	331	66.0	1 M NaOH	[61]
CeO ₂ /CoSe ₂	288	44.0	0.1 M KOH	[59]
CeO _x /NiCo ₂ S ₄ /CC	270	126	1 M KOH	[60]
Cu@CeO ₂ @Ni-Fe-Cr hydroxide	230.8	32.7	1 M KOH	[141]
CeO _x /NiFe-OH/Nickel foam	280 [100 mA cm ⁻²]	43.2	1 M KOH	[144]

2.4. Oxygen Reduction Reaction

Fuel cell is considered as one of the most promising energy-conversion devices due to its environmental friendliness, high efficiency, and reliability. Among them, the low-temperature PEMFCs attract wide attention due to their promising future in practical applications. However, the commercialization of PEMFCs has been limited by the sluggish ORR and the high cost of commercial catalyst Pt. Meanwhile, ORR is also an important cathodic half-reaction in rechargeable metal-air batteries and its slow kinetics severely restricts the power output. Although the Pt-based catalysts are state-of-art for ORR, the scarcity and high price of Pt promote us to develop low-cost and highly active catalysts. Recently, The CeO₂ nanomaterials and CeO₂ containing materials were designed to promote ORR in which the abundant oxygen vacancies on CeO₂ are able to regulate electronic structures of catalysts (Figure 3). Considering the poor conductivity of CeO₂, researchers combine the CeO₂ with functional carbon materials to enhance the conductivity of the composite catalysts. Peng et al. grew CeO₂ nanoparticles in situ on reduced graphene oxide (rGO) and found that the combinations of the high conductivity of rGO and sufficient active sites on CeO₂ enable the nanocomposite to become an efficient electrocatalyst for ORR.^[65] Similar work has proved that the CeO₂/rGO nanocomposite is efficient not only for ORR but also for OER.^[66] In addition to rGO, the C₃N₄ was chosen to composite with CeO₂ to enhance ORR catalytic activity since the pyridinic nitrogen in C₃N₄ functions as a promoter.^[67] Most recently, Pi et al. fabricated CeO₂-encapsulated nitrogen-doped biochars for ORR in Zn/air batteries with remarkable performance.^[68] Experiment combined with DFT illustrates that the Lewis base sites, produced

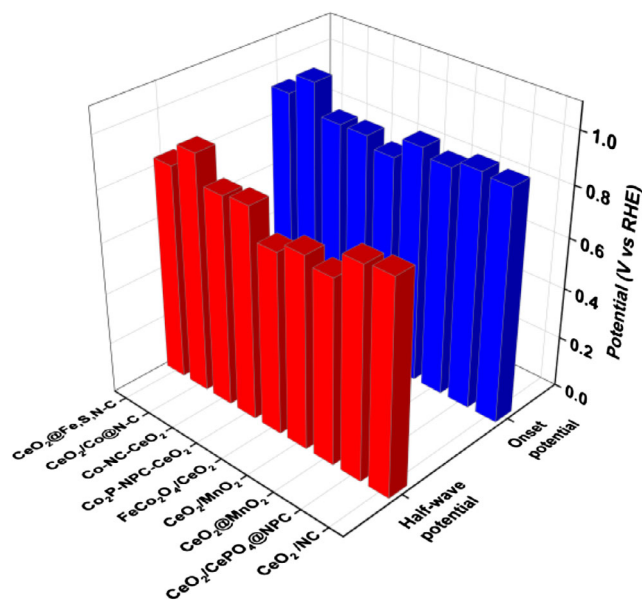


Figure 3. The onset potential and half-wave potential of CeO₂/NC^[68], CeO₂/CePO₄@NPC,^[80] CeO₂@MnO₂,^[75] CeO₂/MnO₂,^[76] FeCo₂O₄/CeO₂,^[53] Co₂P-NPC-CeO₂,^[81] Co-NC-CeO₂,^[77] CeO₂/Co@NC,^[58] and CeO₂@Fe,S,N-C^[82] for ORR.

by pyri-N and oxygen vacancy on CeO₂, remarkably promote the chemisorption of O₂ molecules. It is well known that Pt and Pd locate near the peak of the ORR volcano plot; however, the high expense and scarcity hinders the utilization in large-scale fuel cells.^[69] Constructing the noble metal /CeO₂ catalyst can not only further enhance the catalytic activity and stability of the catalyst but also significantly reduce the loading of noble metal with improved utilization efficiency. Pinheiro et al. reported a hybrid electrocatalyst constructed by Pt nanoparticles and CeO₂ nanorods supported on carbon black for ORR with the aim of application in fuel cells.^[70] As a result, the electrocatalyst shows an improved current and power density than the commercial Pt-based electrocatalysts. Li et al. obtained a similar result and attribute the enhanced performance to that the interaction between CeO₂ and Pt nanoparticles, which prevents surface Pt nanoparticles from aggregation.^[71] Moreover, Du et al. consider that the CeO₂ modifies the electronic density of Pt, which enhances the interactions between Pt and C at the Pt-CeO₂ interface.^[72] In addition, Pt and Pd were also used to fabricate the ORR electrocatalyst by combining CeO₂ and N-doped graphene.^[73,74] Transition metal (oxides) is a kind of low-cost but high active electrocatalyst. Researchers have devoted efforts to build various nanostructures to improve their catalytic activity. A hierarchical CeO₂@MnO₂ core-shell composite and multiple hollow CeO₂ sphere decorated MnO₂ microflower were constructed by Yang et al. to catalyze ORR.^[75–78] The enhanced catalytic performance was simply ascribed to the synergetic effect of CeO₂ and MnO₂. Also, porous hexagonal FeCo₂O₄/CeO₂ heterostructures were prepared. Depending on the abundant interfaces between FeCo₂O₄ and CeO₂, the high ORR catalytic activity is realized.^[53] Doping strategy was considered as an efficient method to improve the performances of electrocatalysts. For both Co-doped

CeO₂ or Co-doped carbon, the ORR catalytic activities of catalysts are significantly improved.^[77,78] Similarly, Sivanantham et al. constructed CeO₂ supported Co in N-doped carbon nanorods and ascribed the improved ORR activity to the synergistic effect of Co and coexistence of Ce³⁺ and Ce⁴⁺ in CeO₂.^[79] Although Yu et al. considered the similar performance that originates from the synergistic effect between CeO₂ nanoparticles and N-doped carbon.^[58] Furthermore, Co₂P and CePO₄ were also chosen to combine with CeO₂ and P, N co-doped carbon to make high performance catalysts for the ORR.^[80–83] Therefore, CeO₂ not only possesses ORR active sites but also it can stabilize noble metals and improve the catalytic performance through electronic interactions. Moreover, the combination of CeO₂ and transition metal is an efficient alternative to develop low-cost and high activity ORR electrocatalysts.

2.5. Methanol/Ethanol Oxidation Reaction

Main direct alcohol fuel cells (DAFCs) have been considered as an attractive fuel device due to their volumetric energy density, environmentally friendliness, and abundant source of methanol or ethanol. The rate of M/EOR on the anode of DAFCs restricts the output power so that it is of great significance to develop efficient electrocatalysts for M/EOR. Similar to ORR, Pt is still the most effective electrocatalyst for M/EOR. However, compared to impressive progress in novel electrocatalysts for ORR, non-Pt catalysts seldom show the desired activity for M/EOR. For the application of Pt-based catalyst, suitable supports will have a key impact on the performance of catalysts and the utilization efficiency of Pt. The interface between active metal and support usually functions as the catalytic active sites due to the special

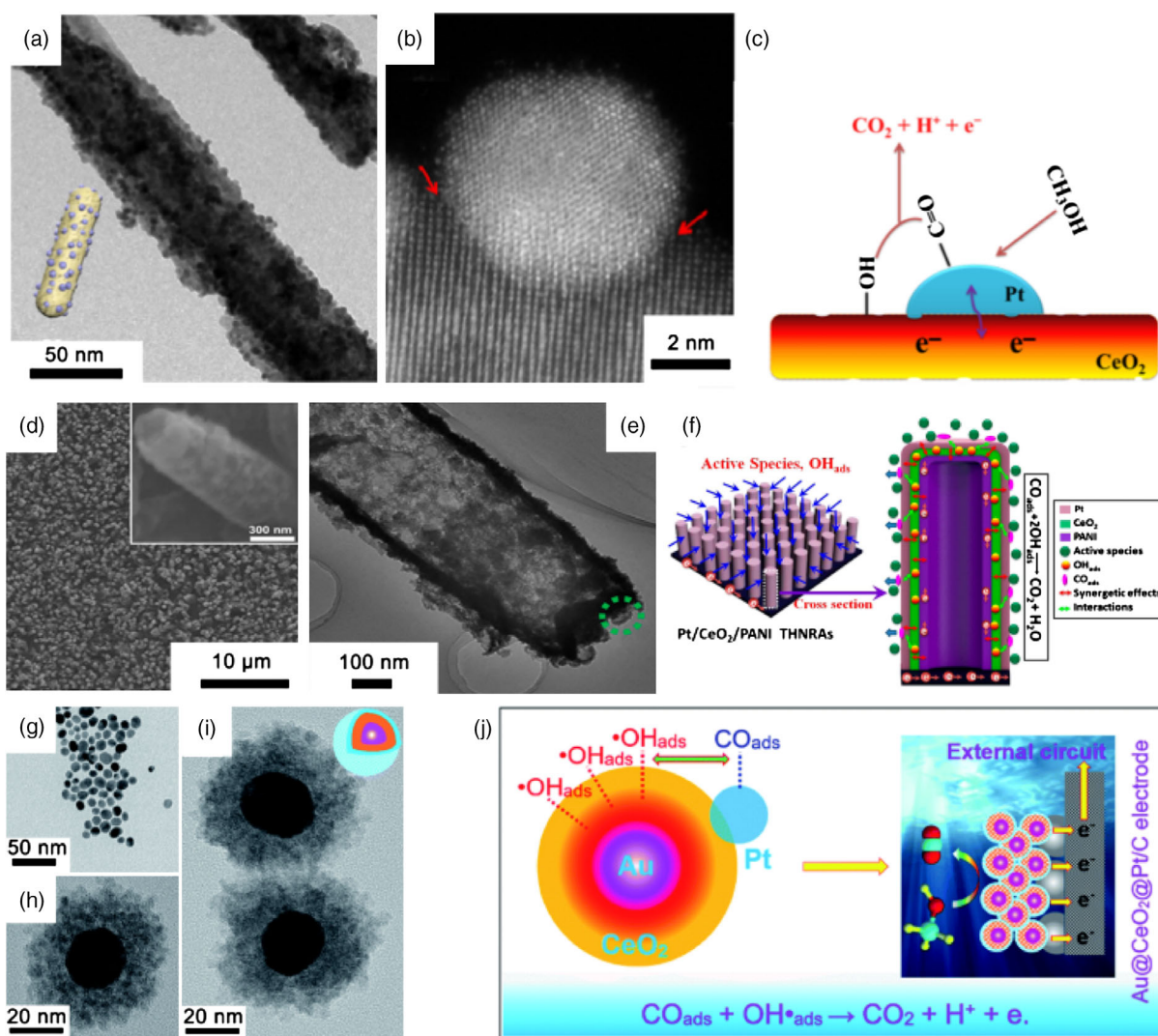


Figure 4. a,b) TEM and aberration-corrected high-angle annular dark-field scanning transmission electron microscopy (HAADF–STEM) images of Pt/CeO₂-P. c) The illustration graph of Pt on oxygen vacancy rich CeO₂. Reproduced with permission.^[84] Copyright 2018, Elsevier. d,e) SEM and TEM image of Pt/CeO₂/PANI hollow nanorods arrays. f) Schematic diagram of Pt/CeO₂/PANI three-layered hollow nanorod arrays. Reproduced with permission.^[90] Copyright 2016, American Chemical Society. g–i) The HRTEM of Au core, Au@CeO₂ core–shell and Au@CeO₂@Pt nanocatalyst. j) The plausible mechanism of the Au@CeO₂@Pt/C electrocatalyst toward methanol oxidation reaction. Reproduced with permission.^[94] Copyright 2019, Royal Society of Chemistry.

lattice and electronic structure. Wang et al. constructed the interface between Pt nanoparticles and CeO₂ rods for MOR (Figure 4a,b).^[84] They discovered that the oxygen vacancy on CeO₂ can supply electrons, which will increase the electron density of Pt by promoting the electron transfer from CeO₂ to Pt, and then, the enhanced catalytic activity and durability of Pt/CeO₂-rod are expected (Figure 4c). Chen et al. synthesized a Ce-modified Pt nanoparticle for MOR and high electrocatalytic activity was achieved (1470 mA mg_{Pt}⁻¹ and 8670 mA mg_{Pt}⁻¹ in acidic and alkaline media, respectively).^[85] DFT calculations indicated that the modification of Ce deforms the Pt surface, which strengthens CO* + OH* bind. The stronger anchoring of OH* removed CO* more easily in the potential determining step, which avoids the CO-poisoning effect easily. Paulo et al. reported that catalytic performances of unsupported Pt nanoparticles for EOR in the acid medium are promoted by adding small amounts of CeO₂ nanoparticles.^[86]

In addition to the influences on the electronic structures, CeO₂ nanoparticles are also able to generate microstrain on the surface Pt, which governs the electrochemical surface area for EOR. Obviously, the size and morphology of CeO₂ have a crucial effect on the catalytic properties of Pt/CeO₂ catalyst. Feng et al. prepared CeO₂ nanoparticles with well-defined morphologies (nanooctahedra, nanosphere, and nanocube) in which the Pt/CeO₂ nanosphere shows the highest catalytic activity for MOR.^[87] Meanwhile, Chen et al. pointed out that the CeO₂ rod exposing (100)/(110) facets are responsible for the higher catalytic activity for MOR than CeO₂ plates and cubes in Pt/CeO₂ catalyst.^[88] The higher Pt nanocrystals trapping ability and metal-support interaction were considered to be responsible for the enhanced performance of Pt/CeO₂ rod. More interestingly, there is also physical interaction between Pt and CeO₂, which allows Pt nanoparticles to highly disperse on CeO₂. Although CeO₂ performs well in Pt/CeO₂ catalysts, the poor conductivity still limits its application. To overcome this issue, researchers composite Pt/CeO₂ with highly conductive multiwalled carbon nanotube (MWCT),^[89] rGO, and polyaniline^[90,91] (Figure 4d–f). In addition, the modification of CeO₂ is also a strategy to develop highly efficient supported Pt-based catalysts. Xie et al. used the Cu-doped CeO₂ as a good support to fabricate Pt/C-Ce_{0.8}Cu_{0.2}O_{2-δ} catalyst and the introduction of Cu increases both the amount of oxygen vacancy and electric conductivity of CeO₂.^[92] ZnO was also doped to Pt/CeO₂ nanofibers to promote surface reaction sites, reactive oxygen species, and the interactions between Pt and CeO₂ for MOR.^[93] Dao et al. constructed Au@CeO₂ core-shell supported Pt catalyst for MOR (Figure 4g–i).^[94] The catalyst showed not only a good catalytic activity but also high CO tolerance because that Au@CeO₂ core-shell structure promotes the oxidation of CO (Figure 4j). In addition to modifying the support, alloying Pt with another transition metal is another efficient method to improve the catalytic performance for M/EOR.^[95–97] Although CeO₂ is often used to construct Pt-based catalysts, the applications of it in non-Pt catalyst are also effective. Chai et al. prepare the Ir₃Sn–CeO₂/C catalyst for EOR and the catalyst was proved to be more active and stable than comparison Pt/C.^[98] Most recently, NiO and rGO were used to composite with CeO₂ aiming at promoting MOR, and enhanced catalytic performance was achieved.^[99,100] Therefore, the introduction of CeO₂ to electrocatalyst stabilizes the active metal to achieve

the well dispersion as well as regulates the electronic of active metals. Since CeO₂ plays a key role in improving the catalytic performance of Pt-based catalysts, introducing CeO₂ into non-Pt catalyst with the aim of enhancing catalytic activity is worth doing.

2.6. CO₂ Reduction Reaction

Electroreduction of CO₂ is another important energy conversion reaction to generate liquid fuels and value-added chemicals. CO₂RR is a multielectron reaction involving different reaction intermediates and a vast number of possible final products (carbon monoxide, formate, formaldehyde, methane, methanol, methanol, and C₂₊ hydrocarbons and oxygenates). Due to the wide variety of reaction products, developing catalysts with high activity and selectivity is the most crucial task, which has attracted the intensive interest of researchers. The active metals of CO₂RR catalyst were classified according to their selectivity: carbon monoxide (Au, Ag, etc.), formate (Pb, Sn, etc.), hydrocarbons (Cu, etc.), and hydrogen (Pt, Ni, etc.). Researchers recently discovered that CeO₂ as an active component or support is beneficial to the CO₂ adsorption and activation. Valenti et al. combined CeO₂ nanoparticles with conductive MWCTs for direct electrocatalytic reduction of CO₂ to formic acid.^[101] Nonstoichiometric Ce^{4+/3+}O^{2-x} reduced sites were proved as essential for the selective CO₂RR. Gao et al. constructed Au–CeO_x interface to enhance CO₂RR (Figure 5a–c).^[17] Experiment combined DFT calculations indicated that Au–CeO_x interface was the active site for CO₂ activation and reduction by promoting the stability of key carboxyl intermediate (*COOH) (Figure 5b,c). Similarly, Zhu et al. manipulated the interface of small-size Au and CeO₂ nanoparticles through adjusting the surface charge of Au and CeO₂, which leads to the utmost utilization of Au and enhancement of CO₂ adsorption.^[102] Varandili et al. synthesized Cu/CeO_{2-x} nanocrystalline heterodimers by a colloidal seeded-growth technique for CO₂RR (Figure 5d–g).^[103] The Cu/CeO_{2-x} heterodimers exhibit high selectivity (≈80%) toward the CO₂RR against the competitive HER and a high Faradaic efficiency for methane (≈54%) (Figure 5h). The catalytic performance was attributed to the formation of sufficient active sites at the interface, which strengthens the stabilization of intermediates CHO* through bidentate adsorption at Cu and oxygen vacancy on CeO_{2-x} site simultaneously. The interface effect not only promotes the CO₂RR but also strongly inhibits the competitive HER process. To further study the interaction between Cu and CeO₂ support, Wang et al. predicted through theoretical calculations that the single atomic Cu substitution in CeO₂ (110) surface generates three oxygen vacancies around Cu site, which are highly active catalytic sites for the initial CO₂ adsorption and subsequent activation.^[18] Cu-doped mesoporous nanorods, which partially expose the (110) plane, were targetedly synthesized and its catalytic performance was consistent with the theoretical calculations.

Wu et al. reported CeO₂ doped with Cu⁺ for CO₂RR and it shows the high faradaic efficiency for ethylene (47.6%) with long-term durability.^[104] Furthermore, the methane selectivity is improved by comparing with 0D Cu. In this catalyst, CeO₂ function as the stabilizer for Cu⁺. So, for Cu-based

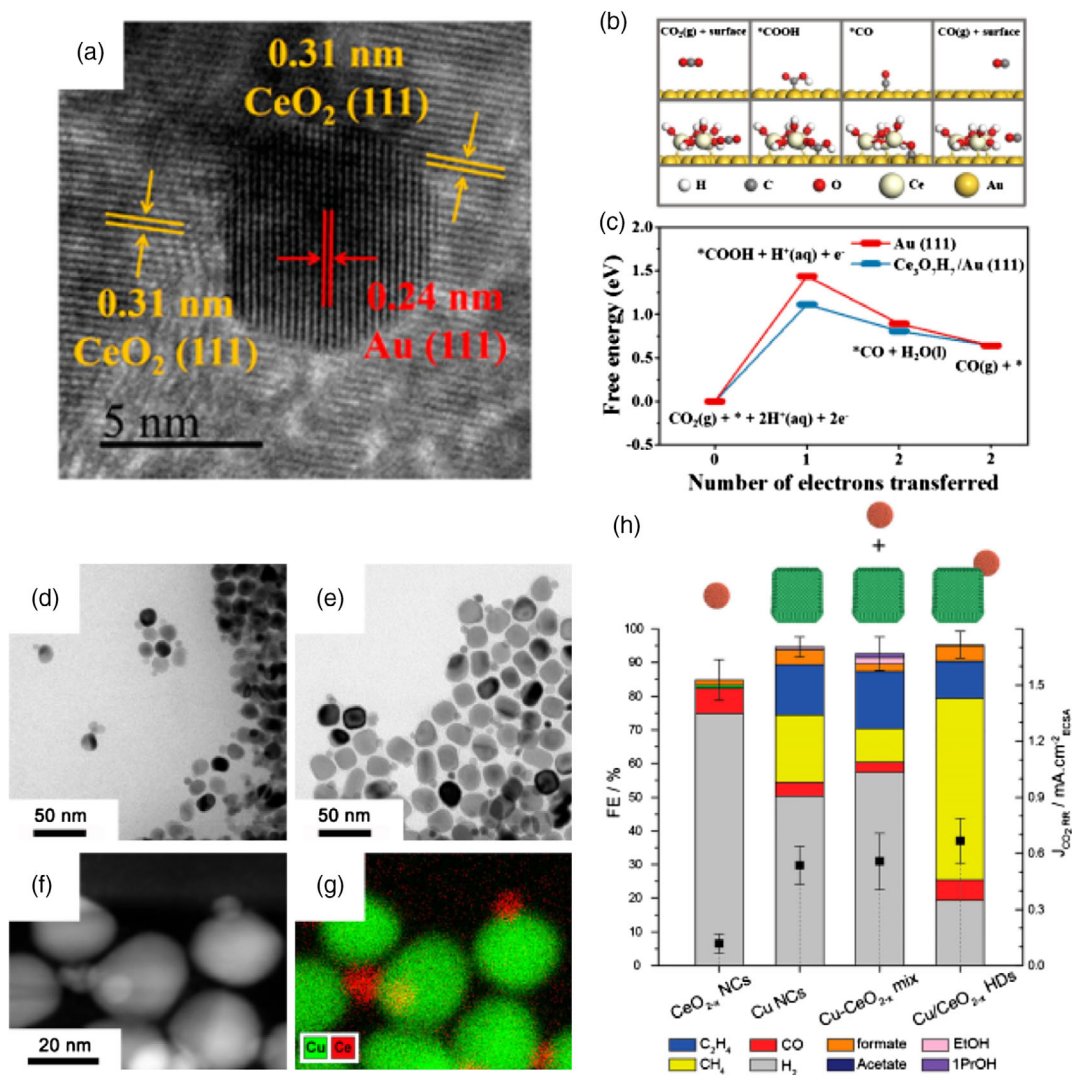


Figure 5. a) HRTEM image of Au–CeO_x/C catalyst. b,c) DFT calculation of CO₂RR at 0V versus RHE on Au (111) surfaces. Reproduced with permission.^[17] Copyright 2017, American Chemical Society. d,e) Bright-field TEM image of Cu/CeO_{2-x} heterodimers formed by injection of 0.1 and 0.2 mmol of CuOAc. f,g) HAADF–STEM image with the corresponding energy dispersive X-ray elemental maps of Cu and Ce in Cu (24 nm)/CeO_{2-x} heterodimers. h) Faradaic efficiencies and CO₂RR partial current-densities for Cu/CeO_{2-x} heterodimers, Cu–CeO_{2-x} mix, Cu nanocrystals, and CeO_{2-x} nanocrystals. Reproduced with permission.^[103] Copyright 2019, American Chemical Society.

electrocatalysts, the CeO₂ can not only enhance the activity but also improve the selectivity of methane. In addition to Cu, transition metal oxides are also used as active components of catalysts for CO₂RR. Zhang et al. constructed Co₃O₄–CeO₂/low graphitic carbon, which can efficiently reduce CO₂ to formate at only –0.31 V versus reversible hydrogen electrode (RHE).^[105] They indicate that the oxygen vacancies enriched by the addition of Co₃O₄ are the key reason for the inhibited HER, enhanced activity, and stable formate selectivity. In summary, for electrocatalytic CO₂ reduction, CeO₂ not only enhances the activity but also has a certain impact on the selectivity of CO₂RR and it depends on the specific active components. Therefore, based on these results, CeO₂ is the ideal component to fabricate CO₂RR catalysts through the combination with other transition metal based materials.

2.7. N₂ Reduction Reaction

NH₃ is considered as one of the most important industrial chemicals and it is mainly synthesized from N₂ through harsh reaction conditions (Haber–Bosch process), which shows a tedious reaction process and high cost. Electroreduction of N₂ realizes the reaction in the facile environment. The N₂ reduction reaction (NRR) involves a six-electron transfer process and multiple intermediates due to the different reaction mechanisms. Similar to the CO₂RR, HER is also the main competing reaction, which makes selectivity a great challenge. CeO₂ itself is selected to be the catalysts for NRR. Xu et al. performed NRR on CeO₂ nanorods without any modification and discovered that CeO₂ with oxygen vacancy is catalytic active for NRR.^[106] Meanwhile, Xie et al. also anchored ultras-small CeO₂ on rGo to improve the

conductivity of CeO₂.^[107] Many reports point that the electrocatalytic activity of the reported electrocatalyst is related to the abundant oxygen vacancies in CeO₂. Zhang et al. synthesized Cu-doped CeO₂ nanorods and found that Cu doping can effectively enrich the concentration of multiple oxygen vacancies, which significantly enhances NRR activity.^[108] Similarly, Xie et al. prepared Cr-doped CeO₂ to increase the oxygen vacancies for NRR and an enhanced activity was achieved at −0.7 V versus RHE^[109] Amorphous materials are more catalytically active to some degree because they usually exhibit “dangling bonds”. CeO_x has been applied to induce the amorphization of Au nanoparticles on rGO by Li et al.^[110] The amorphous Au shows strong structural distortion with more active sites for NRR, which shows higher ammonia yield (8.3 μg h^{−1} mg^{−1} cat) and Faradaic efficiency (10.10%) at −0.2 V versus RHE than the crystalline counterpart. Similarly, Lv et al. prepared an amorphous Bi₄V₂O₁₁/CeO₂ hybrid through a spinneret electrospinning method. The CeO₂ functions as a trigger to induce the amorphous phase and promotes the interfacial charge transfer by build band alignment with Bi₄V₂O₁₁.^[111] In addition, CeO₂ supported single metal atoms become potential electrocatalysts for NRR. To prove it, Qi et al. conducted DFT calculations on transition metal atomic catalysts supported by stepped CeO₂.^[112] The screening results showed that Nb, V, Ru, Mo, W, and Os atoms supported on CeO₂ are possible NRR catalysts. Therefore, both experimental and theoretical calculations indicate that CeO₂ plays a key role to enhance the catalytic activity for NRR, and CeO₂-based NRR catalyst deserves more attention in the future due to their potential.

3. CeO₂-Based Photocatalyst

3.1. Hydrogen Evolution Reaction

In addition to the electrically driven water splitting reaction, the photocatalytic HER is another promising approach to produce H₂ by an environment-friendly way. Semiconductor photocatalysis for efficient water splitting has attracted lots of research in which the narrow bandgap and imperative photoredox behavior are fundamental required properties. Because of the easy conversion between Ce³⁺ and Ce⁴⁺ and rich oxygen vacancies, nanostructured CeO₂ often was used as support or composite material to enhance photocatalytic activity.^[113,114] Dong et al. prepared CeO₂ nanorods and found that the bare CeO₂ without compositing any other active component shows photocatalytic activity.^[115] The H₂ production rate of 5.02 μmol g^{−1} h^{−1} under solar light irradiation was achieved, and the photocatalytic activity was related to the conversion of Ce³⁺/Ce⁴⁺ and oxygen vacancies. Krishnan et al. reduced the bandgap of CeO₂ to 2.5 by adding Fe₂O₃, which endows CeO₂ absorption in the visible region, enhanced charge separation, and low rate of electron–hole pair recombination.^[116] CdS is an extensively studied photocatalyst due to its appropriate bandgap (≈2.4 eV) and superior sensitizing properties. Compositing CdS with CeO₂ is an approach to further improve the photocatalytic activity. Zheng et al. fabricated ultrathin CdS shell-sensitized S-doped CeO₂ hollow spheres, which exhibits remarkably enhanced photocatalytic activity for HER (1147.2 μmol g^{−1} h^{−1}) under visible light illumination

(Figure 6a,b).^[117] The oxygen vacancies in S-doped CeO₂ reduced bandgap of catalysts and the CdS sensitization effect promotes the interface carrier separation and transfer, which results in superior photocatalytic performance (Figure 6c). CdS quantum dot (QD) is a promising material for photocatalyst due to its unique small size (<10 nm), short effective charge transfer length, suitable bandgap, and extensive light-harvesting. Ma et al. constructed 0D/1D CdS QDs/CeO₂ nanorod heterojunction and noted the enhanced photocatalytic performance.^[118] The 0D/1D CdS QDs/CeO₂ heterojunctions provide stronger electronic conductivity, improved light-harvesting, and enhanced photoresponse, which was beneficial for photocatalysts. Z-scheme heterojunction was widely studied because it enhances the separation efficiency of photogenerated electron–hole pairs and the reduction capacity of electrons participating in HER. The Z-scheme between CdS QDs and CeO₂ nanorods was a key factor in the increased photocatalytic performance. Moreover, Sultana synthesized ternary nanoheterostructure, CeO₂ nanosheets supported CdSQDs and Au nanoparticles.^[119] The Au nanoparticle incorporated into the interface between CeO₂ and CdS QDs is a mediator, which injects hot electrons through the LSPR (light-induced surface plasmon resonance) effect, which is responsible for the enhancement in photocatalytic performance. Compared with CeO₂ supported QDs materials, CeO₂ QD embedded in porous carbon nanotubes (CNTs) by a versatile biotemplate method is also achieved.^[120] In addition, Qian et al. synthesized in situ CeO₂-CuO QDs heterojunction on graphene and the p-type CuO/n-type CeO₂ heterojunction show a superior photocatalytic performance (H₂ evolution rate, 2481 μmol g^{−1} h^{−1}).^[121] The pn heterojunctions in semiconductor-based photocatalysts is essential in promoting H₂ production. Swain et al. constructed p-MoS₂/n-CeO₂ heterojunction toward solar hydrogen production.^[122] They found that the pn heterojunction provides an internal electric field to promote the photogenerated charge separation and transfer. A quaternary Cu₂ZnSnS₄ nanoparticle decorated CeO₂ pn heterojunction was reported by Sridharan et al., which reaches hydrogen production efficiency of 2930 μmol g^{−1} h^{−1}.^[123] CeO₂ coupled Cu₂ZnSnS₄ induces the visible light absorption and separation, the transmission of photoinduced charge carriers, as well as impedes the rapid electron–hole pair recombinations. Wang et al. designed 0D/2D Mn_{0.2}Cd_{0.8}S/CeO₂ directed Z-scheme and photocatalytic H₂ production rate of 8.73 mmol g^{−1} h^{−1} was obtained in Na₂S/Na₂SO₃ aqueous solution.^[124] CeO₂/CeVO₄/V₂O₅ was prepared to induce Z-scheme-charge-transfer and drive photocatalytic degradation coupled with H₂ generation.^[125] The CeVO₄ nanoparticles function as a conductive channel to transfer photogenerated carriers, as redox centers to facilitate the transfer of photogenerated electrons and enhance the separation efficiency of electron–hole pair. Graphitic carbon nitride (g-C₃N₄) was considered as a promising candidate material for photocatalyst due to its medium bandgap (≈2.7 eV) and excellent photocatalytic stability. A new strategy that combines g-C₃N₄ with CeO₂ has been constructed for efficient water splitting. Liu et al. prepared g-C₃N₄ supported CeO₂ nanocomposites for photocatalytic HER and the hydrogen generation rate is 0.83 mmol g^{−1} h^{−1} under visible light illumination, which was ascribed to the interfacial effects caused more visible light absorbance and enhanced electron transfer.^[126] Waqas et al. fabricated N-bonded CeO_{2-x}/g-C₃N₄ hollow structure

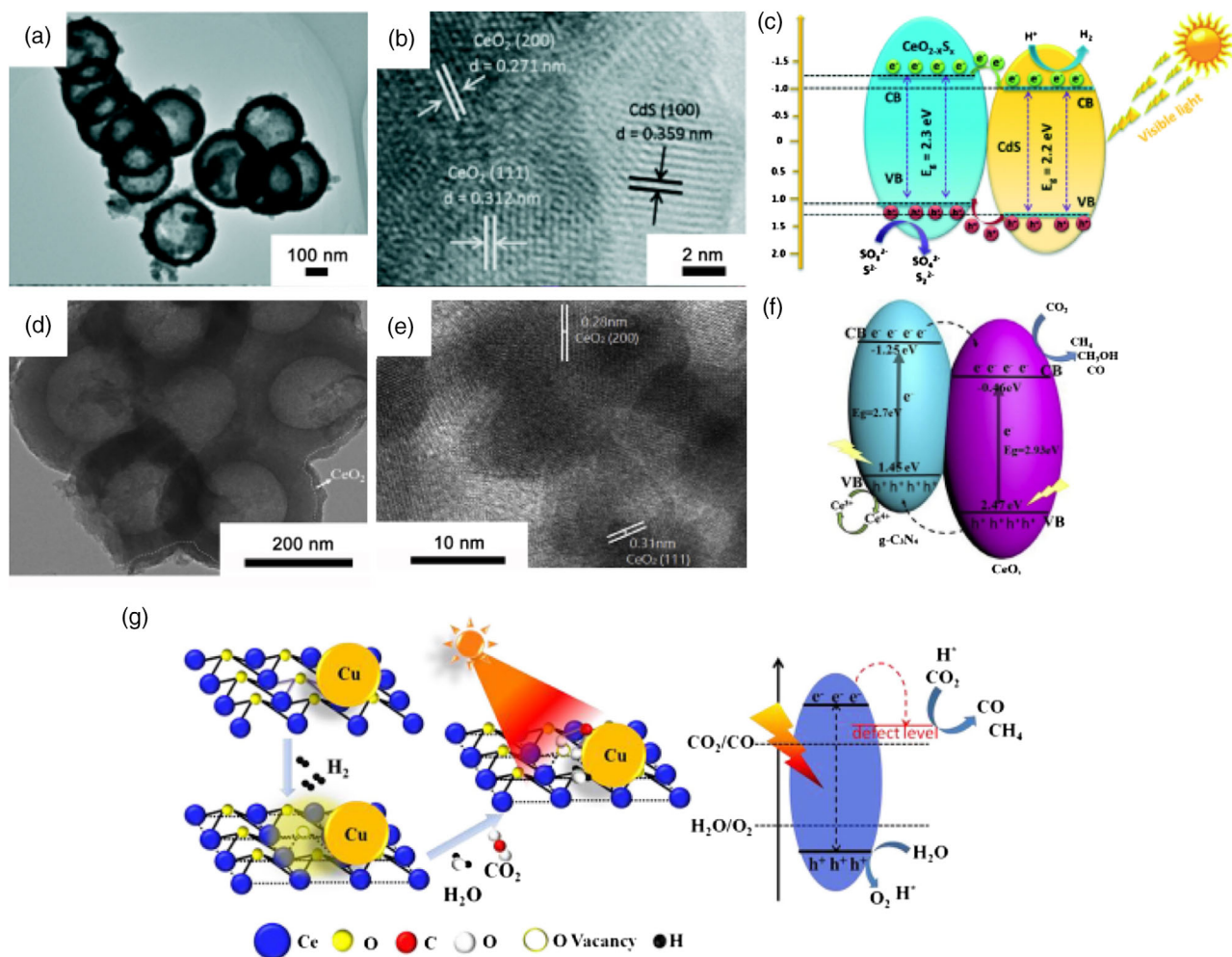


Figure 6. a,b) TEM and HRTEM images of CeO_{2-x}S_x@CdS composite. c) Schematic diagram of the proposed charge carrier transfer and H₂ evolution mechanism over the CeO_{2-x}S_x@CdS photocatalyst under visible light irradiation. Reproduced with permission.^[117] Copyright 2019, Royal Society of Chemistry. d,e) TEM and HRTEM images of g-C₃N₄@CeO₂. f) Schematic illustration of band structure diagram and photoinduced carriers transfer of g-C₃N₄@CeO₂ under visible light irradiation. Reproduced with permission.^[132] Copyright 2019, Elsevier. g) Scheme of possible mechanism of CO₂ reduction on Cu/CeO_{2-x}. Reproduced with permission.^[133] Copyright 2019, American Chemical Society.

by incorporating cyanamide molecules.^[127] In this photocatalyst, hollow structure enhanced light-harvesting ability; Ce³⁺ functioned as optically active sites; inorganic/organic interfaces boosted the separation efficient of minority carrier. To further improve the photocatalytic activity for the water splitting, a ternary composite, CeO₂ nanocrystal-modified layered MoS₂/g-C₃N₄ was constructed.^[128] The well-matched energy-level position and efficient charge separation caused by electron transfer processes between Ce⁴⁺/Ce³⁺ pairs and heterostructures were responsible for the superior. Moreover, the interfacial electronic interaction and Ce³⁺ species promotes adsorption capacity and decreases energy barrier for reactant H₂O adsorption, which is beneficial for the water splitting. Similarly, CeO₂@Ni₄S₃/g-C₃N₄ synthesized by Yu et al. exhibits an enhanced photocatalytic activity under the visible light.^[129] Therefore, the CeO₂ supported QDs materials, constructed pn heterojunction, and the Z-Scheme, etc. have exhibited superior photocatalytic performance due to the improved light harvesting, enhanced

charge separation, and impeding the rapid electron–hole pair recombination. In conclusion, CeO₂ can not only play the role of active sites for photocatalytic HER but also more importantly, it can regulate the bandgap, enhance light harvesting, and impede the rapid electron–hole pair recombination of catalysts, which closely related to photocatalytic HER activity (Table 3).

3.2. CO₂ Reduction Reaction

Recently, photocatalytic CO₂RR has caught the researchers' eyes because it can produce value-added chemicals and energy-rich fuel while mitigating CO₂ emission. Many strategies have been applied to fabricate nanomaterials for CO₂RR, and compositing CeO₂ with traditional photocatalytic material is an effective method to promote CO₂ conversion.^[101] Li et al. designed and synthesized mesostructured CeO₂/g-C₃N₄ to promote CO₂ photoreduction and the main product is CO and CH₄.^[130] The

Table 3. Summary of the HER catalytic property of various CeO₂-based photocatalysts.

Photocatalyst	H ₂ evolution rate [$\mu\text{mol h}^{-1} \text{g}^{-1}$]	Ref.
CdS QDs/CeO ₂	101	[118]
Pt/CeO ₂	19 700	[113]
CeO ₂ QDs/C	582	[120]
Cu ₂ ZnSnS ₄ /CeO ₂	2930	[123]
N-CeO _{2-x} /g-C ₃ N ₄	43	[127]
CeO _{2-x} S _x @CdS	1147	[117]
Mn _{0.2} Cd _{0.8} S/CeO ₂	8730	[124]
CeO ₂ -CuO QDs/graphene	2481	[121]
CeO ₂ -Au-CdS QDs	12 475	[119]
CeO ₂	5	[115]
CeO ₂ /g-C ₃ N ₄	830	[126]
CeO ₂ @Ni ₄ S ₃ /g-C ₃ N ₄	3740	[129]
CeO ₂ -Fe ₂ O ₃	584 [$\mu\text{mol h}^{-1}$]	[116]
p-MoS ₂ /n-CeO ₂	721 [$\mu\text{A cm}^{-2}$]	[122]

enhanced photocatalytic performance is ascribed to the synergistic effect of mutual activations in CeO₂ and g-C₃N₄. Han et al. prepared a series of CeO₂-modified C₃N₄ and their band structures have been carefully revealed by both theoretical calculations and experimental characterizations.^[131] It is noted that the CeO₂-modified C₃N₄ matches the energy, enhances the absorption in the visible region, and promotes the separation of photogenerated electron-hole pair, which improves the photocatalytic performance. Liang et al. synthesized the g-C₃N₄@CeO₂ photocatalyst with hollow heterostructures and rich oxygen vacancies. CO₂ has been selectively converted to CH₄, CH₃OH, and CO (Figure 6d-f).^[132] The oxygen vacancies can facilitate charge separation and transfer. Meanwhile, the hollow frame improves the light efficiency due to the multiple reflections in the chamber. Wang et al. enriched and stabilized oxygen vacancies on CeO₂ by introducing Cu and as expected, the Cu/CeO_{2-x} showed the enhanced photocatalytic activity for CO yield.^[133] The oxygen vacancies not only promote the separation and transfer of photogenerated charge carriers but also enhance the visible light absorption (Figure 6g). Ag is a catalytically active metal for CO₂ reduction whether in electrocatalysis or photocatalysis. Wang et al. synthesized order mesoporous CeO₂ and constructed g-C₃N₄/Ag/CeO₂ composite. The ordered mesostructure is a merit for the CO₂ adsorption and migrations, where the g-C₃N₄ nanosheets can protect the Ag nanoparticles from photocorrosion to further boost the CO₂ photoreduction.^[134] TiO₂ possesses many advantages such as high stability, nontoxicity, and low cost as a photocatalyst. Seeharaj et al. fabricated TiO₂/rGO/CeO₂ heterojunction with a modified surface to convert CO₂ to CH₃OH and C₂H₅OH.^[135] The strong connection and high interfacial contact area between TiO₂ nanosheets, rGO, and CeO₂ promote the photogenerated charge carriers to react with adsorbed species, and the heterojunction effectively hindered electron-hole recombination. The rod-like attapulgite was used to modify spindle-structured CeO₂ to enhance photocatalytic performance for the CO₂ reduction.^[136] The accumulation of CeO₂ was

inhibited by the introduction of attapulgite and thereby the active sites for CO₂ conversion were increased. Moreover, a ternary photocatalyst consists of In₂O₃, CeO₂, and HCl treated attapulgite also present high activity for CO and CH₄ yields.^[137] Doping is also an effective approach to enhance the photocatalytic activity of CeO₂ by extending the spectral response range and improving electronic conductivity.^[138] In summary, oxygen vacancies not only promote the separation and transfer of photogenerated charge carriers but also enhance visible light absorptions. Therefore, abundant oxygen vacancies on CeO₂ and the formed heterostructure with other traditional photocatalytic materials results in the CeO₂-based photocatalyst high efficiency for CO₂ conversion.

4. Theoretical Explorations of CeO₂-Based Catalysts

In recent years, the significant contribution of CeO₂ in catalysis has been proved by many experiments. In the meantime, the theoretical calculations have also been applied in these electrocatalysts to supply more insights into improved performance. The intrinsic electroactivity of CeO₂ and the contribution to the electrocatalysis as catalyst support have been revealed by theoretical calculations in recent years.

The flexible switching between Ce³⁺ and Ce⁴⁺ due to the formation of oxygen vacancy formation is usually considered as the key reason for the high intrinsic electroactivity. In previous works, Huang et al. have studied the native defect formation in CeO₂ based on the DFT with repulsive potential (DFT + U) method.^[139] To reduce the calculation error induced by overlaps of valence-core charge density, they have selected the nonlinear core correction (NLCC) method for 4f levels in lanthanides. They have confirmed the low energy barrier of 0.39 eV for the formation of an oxygen vacancy. The identified negative U of oxygen vacancy further supports the excellent photocatalytic performance. Later in another work by Zhu et al, the high mobility of Ce with the formation of CeO₂ nanoclusters has been identified by the atomic-resolution electron energy-loss spectroscopic mapping.^[140] The oxygen-exchange mechanism further supports the ability of mobile Ce⁴⁺ to carry oxygen or create oxygen vacancies to enhance oxygen transport. These preliminary works have supplied insightful information on the intrinsic activity of CeO₂. On the other side, CeO₂ plays a different role in catalysts for different material systems. In our previous works, we have successfully constructed the CeO₂-based composite electrocatalysts for OER.^[141] Within such an interfacial structure, CeO₂ supplies the abundant 4f orbitals in a wide range as the "electron transfer expressway" to facilitate the electron transfer based on the d-f couplings between CeO₂ and NiFeLDH. This electronic environment is highly beneficial for high-speed charge transfer to promote the OER. Meanwhile, CeO₂ also plays as a good atomic catalyst support for Rh single atomic catalyst.^[142] CeO₂ shows a good coupling effect with the anchoring Rh atoms to stabilize the surface atom, which also further optimizes the binding strength of CH₄ to achieve the oxidation process. In recent years, the theoretical investigation of CeO₂ is usually based on the transition

metal modification. For example, Wang et al. have reported the formation of oxygen vacancies in Fe, Co, and Ni-doped CeO₂ as well as their electroactivity for CH₄ activation.^[143] They have systematically revealed the oxygen vacancy formation in (111) and (110) surfaces of the doped-CeO₂ surfaces. They also compared the CH₄ adsorption and C–H dissociation process based on the activation energy barriers. They concluded that the formation of oxygen vacancies is facilitated by the substitution of transition metals in the CeO₂, which is more energetically preferred than the adsorption and insertions of transition metals.

Although explorations on the CeO₂-based catalysts have been reported, the in-depth discussions from theoretical perspectives, especially for the photocatalytic performance, are still lacking. This is attributed to the challenge of accurate calculation in electronic structures of rare earth metal materials. Meanwhile, different combinations between CeO₂ and other material systems also supply significant references to the understanding of catalytic mechanisms. In the future, more efforts in the theoretical investigations of CeO₂-based catalysts are still highly needed.

5. Conclusion, Opportunities, and Outlook

This review systematically summarizes the application of CeO₂-based materials in the electrocatalytic and photocatalytic energy conversion-related reactions (HER, OER, ORR, M/EOR, CO₂RR, and NRR). CeO₂ was extensively used to composite with other catalytically active components to construct the special structure with enhanced electro(photo)catalytic performance. CeO₂ mainly disperse and anchor active component nanoparticles to increase the number of active sites, which demonstrates a strong electronic interaction with active components to achieve the regulation of their electronic structures, aiming to improve the intrinsic activity. The two important features of CeO₂, abundant oxygen vacancies and flexible transitions between Ce³⁺ and Ce⁴⁺, play a key role to improve the electro(photo)catalytic activity of catalysts. Furthermore, we discussed the role of CeO₂ in different electro(photo)catalysts in detail. The activity and stability of different catalysts including novel metal, transition metals, transition metal phosphides, and transition metal nitrides catalysts are enhanced by compositing CeO₂ since it tends to regulate and optimize the electronic structure of the catalyst. The optimized reactant, intermediate, and product adsorption/desorption energy caused by modulating the electronic structure of catalysts leads to a promoted electrocatalytic performance. CeO₂ can not only play the role of active sites for photocatalysts but also more importantly, it can regulate the bandgap, enhance light harvesting, and impede the rapid electron–hole pair recombination of catalysts, which is closely related to the photocatalytic activity. However, there are still several challenges in the understanding and commercial application of CeO₂-based electro(photo)catalysts.

Therefore, to further rationally design and develop more efficient CeO₂-based electro(photo)catalysts with better performance, we believe the following aspects should be focused on: 1) further study the effect of oxygen vacancy and Ce³⁺/Ce⁴⁺ ratio on catalytic activity combining theoretical calculations and in situ technologies. Most of the current works only qualitatively reveal that oxygen vacancy and Ce³⁺ are beneficial to catalytic activity,

the direct evidence by advanced in situ technology, and theoretical calculations are still needed. A more accurate and in-depth understanding of this structure-activity relationship is of great significance for researchers to design and fabricate highly effective electro(photo)catalysts; 2) precise synthesis of CeO₂ with a controlled amount of oxygen vacancies and the ratio of Ce³⁺/Ce⁴⁺. Precise synthesis is the goal pursued in the field of material synthesis. It is not only vital to enhance catalytic performance but also to provide valuable references for our research on catalytic mechanisms; 3) based on the understanding of the effect of structure on catalytic performance, efficiently synthesized CeO₂-based materials with the specific structure are critical to the catalytic reaction. We should aim to conversely design and build specific nanostructures like hydrophilic/hydrophobic surface, array, core–shell, porous, and hollow structures, etc. to create more active sites and enhance the mass transfer for specific reactions; and 4) improve the conductivity of CeO₂-based materials to promote the transfer of electrons in the reaction by doping strategies, compositing highly conductive materials, and directly growing active materials on the conductive substrates (carbon cloth, metal foam, etc.).

In summary, although CeO₂-based catalysts have shown good performances in electro(photo)catalysis, there is still untapped potential for the improvement of properties and commercial applications. With the continuous efforts devoted by researchers and engineers, we believe that CeO₂-based catalysts will activate and convert energy-related small molecules more efficiently and be applied in industrial productions in the future.

Acknowledgements

The authors gratefully acknowledge the support from the China National Funds for Excellent Young Scientists (Grant No.: 21522106) and National Natural Science Foundation of China (Grant No.: 21971117; 21771156), 111 Project (B18030) from China, and the Open Funds (RERU2019001) of the State Key Laboratory of Rare Earth Resource Utilization, the Functional Research Funds for the Central Universities, Nankai University (ZB19500202), the Shenzhen Fundamental Research Project (Grant No.: JCY20170818100717134), and the Early Career Scheme (ECS) fund (Grant No.: PolyU 253026/16P) from the Research Grant Council (RGC) in Hong Kong.

Conflict of Interest

The authors declare no conflict of interest.

Keywords

CeO₂-based materials, electrocatalysts, electronic interaction, oxygen vacancy, photocatalysts

Received: November 2, 2020
Revised: November 28, 2020
Published online: January 8, 2021

- [1] S. Chu, A. Majumdar, *Nature* **2012**, 488, 294.
[2] Z. W. Seh, J. Kibsgaard, C. F. Dickens, I. Chorkendorff, J. K. Nørskov, T. F. Jaramillo, *Science* **2017**, 355.

- [3] M. B. Ross, P. De Luna, Y. Li, C.-T. Dinh, D. Kim, P. Yang, E. H. Sargent, *Nat. Catal.* **2019**, 2, 648.
- [4] I. Roger, M. A. Shipman, M. D. Symes, *Nat. Rev. Chem.* **2017**, 1.
- [5] M. K. Debe, *Nature* **2012**, 486, 43.
- [6] D. R. MacFarlane, P. V. Cherepanov, J. Choi, B. H. R. Suryanto, R. Y. Hodgetts, J. M. Bakker, F. M. Ferrero Vallana, A. N. Simonov, *Joule* **2020**, 4, 1186.
- [7] G. Zhao, K. Rui, S. X. Dou, W. Sun, *Adv. Funct. Mater.* **2018**, 28, 1803291.
- [8] F. Yang, X. Bao, P. Li, X. Wang, G. Cheng, S. Chen, W. Luo, *Angew. Chem. Int. Ed.* **2019**, 58, 14179.
- [9] J. Stacy, Y. N. Regmi, B. Leonard, M. Fan, *Renew. Sustain. Energy Rev.* **2017**, 69, 401.
- [10] L. Huang, X. Zhang, Q. Wang, Y. Han, Y. Fang, S. Dong, *J. Am. Chem. Soc.* **2018**, 140, 1142.
- [11] Y. Wan, J. Xu, R. Lv, *Mater. Today* **2019**, 27, 69.
- [12] J. Wang, X. Xiao, Y. Liu, K. Pan, H. Pang, S. Wei, *J. Mater. Chem. A*, **2019**, 7, 17675.
- [13] S. Xie, Z. Wang, F. Cheng, P. Zhang, W. Mai, Y. Tong, *Nano Energy* **2017**, 34, 313.
- [14] G. Lu, H. Zheng, J. Lv, G. Wang, X. Huang, *J. Power Source* **2020**, 480, 229091.
- [15] W. Gao, D. Wen, J.C. Ho, Y. Qu, *Mater. Today Chem.* **2019**, 12, 266.
- [16] M. Melchionna, P. Fornasiero, *Mater. Today* **2014**, 17, 349.
- [17] D. Gao, Y. Zhang, Z. Zhou, F. Cai, X. Zhao, W. Huang, Y. Li, J. Zhu, P. Liu, F. Yang, G. Wang, X. Bao, *J. Am. Chem. Soc.* **2017**, 139, 5652.
- [18] Y. Wang, Z. Chen, P. Han, Y. Du, Z. Gu, X. Xu, G. Zheng, *ACS Catal.* **2018**, 8, 7113.
- [19] M. M. Liu, Z. Y. Ji, X. P. Shen, H. Zhou, J. Zhu, X. L. Xie, C. S. Song, X. L. Miao, L. R. Kong, G. X. Zhu, *Eur. J. Inorg. Chem.* **2018**, 2018, 3952.
- [20] X. Gao, G. Yu, L. Zheng, C. Zhang, H. Li, T. Wang, P. An, M. Liu, X. Qiu, W. Chen, W. Chen, *ACS Appl. Energy Mater.* **2019**, 2, 966.
- [21] T. Gao, J. Yang, M. Nishijima, H. A. Miller, F. Vizza, H. Gu, H. Chen, Y. Hu, Z. Jiang, L. Wang, L. Shuai, M. Qiu, C. Lei, A. Zhang, Y. Hou, Q. He, *J. Electrochem. Soc.* **2018**, 165, F1147.
- [22] E. Demir, S. Akbayrak, A. M. Önal, S. Özkar, *ACS Appl. Mater. Interfaces* **2018**, 10, 6299.
- [23] M. Akbayrak, A. M. Önal, *J. Electrochem. Soc.* **2019**, 166, H897.
- [24] Z. Sun, J. Zhang, J. Xie, M. Wang, X. Zheng, Z. Zhang, X. Li, B. Tang, *Dalton Trans.* **2018**, 47, 12667.
- [25] Y. Xiao, W. Wang, Q. Wu, *Int. J. Hydrogen Energy* **2020**, 45, 3948.
- [26] S. Jiang, R. Zhang, H. Liu, Y. Rao, Y. Yu, S. Chen, Q. Yue, Y. Zhang, Y. Kang, *J. Am. Chem. Soc.* **2020**, 142, 6461.
- [27] L. Xiong, J. Bi, L. Wang, S. Yang, *Int. J. Hydrogen Energy* **2018**, 43, 20372.
- [28] R. Zhang, X. Ren, S. Hao, R. Ge, Z. Liu, A. M. Asiri, L. Chen, Q. Zhang, X. Sun, *J. Mater. Chem. A* **2018**, 6, 1985.
- [29] L. Zhang, X. Ren, X. Guo, Z. Liu, A. M. Asiri, B. Li, L. Chen, X. Sun, *Inorg. Chem.* **2018**, 57, 548.
- [30] B. Zhang, H. Qin, L. Diao, N. Zhao, C. Shi, E. Liu, C. He, *J. Catal.* **2019**, 377, 582.
- [31] M. Zhao, Y. Li, H. Dong, L. Wang, Z. Chen, Y. Wang, Z. Li, M. Xia, G. Shao, *Catalysts* **2017**, 7, 197.
- [32] Z. Sun, J. Zhang, J. Xie, X. Zheng, M. Wang, X. Li, B. Tang, *Inorg. Chem. Front.* **2018**, 5, 3042.
- [33] M. Bellini, M. V. Pagliaro, A. Lenarda, P. Fornasiero, M. Marelli, C. Evangelisti, M. Innocenti, Q. Jia, S. Mukerjee, J. Jankovic, L. Wang, J. R. Varcoe, C. B. Krishnamurthy, I. Grinberg, E. Davydova, D. R. Dekel, H. A. Miller, F. Vizza, *ACS Appl. Energy Mater.* **2019**, 2, 4999.
- [34] H. Yu, E. S. Davydova, U. Ash, H. A. Miller, L. Bonville, D. R. Dekel, R. Maric, *Nano Energy* **2019**, 57, 820.
- [35] V. Yarmiyev, M. Alesker, A. Muzikansky, M. Zysler, D. Zitoun, *J. Electrochem. Soc.* **2019**, 166, F3234.
- [36] N. Ralbag, E. S. Davydova, M. Mann-Lahav, P. Cong, J. He, A. M. Beale, G. S. Grader, D. Avnir, D. R. Dekel, *J. Electrochem. Soc.* **2020**, 167, 054514.
- [37] H. A. Miller, F. Vizza, M. Marelli, A. Zadick, L. Dubau, M. Chatenet, S. Geiger, S. Cherevko, H. Doan, R. K. Pavlicek, S. Mukerjee, D. R. Dekel, *Nano Energy* **2017**, 33, 293.
- [38] H. A. Miller, A. Lavacchi, F. Vizza, M. Marelli, F. Di Benedetto, F. D. Y. AcapitoPaska, I. Y. Paska, M. Page, D. R. Dekel, *Angew. Chem. Int. Ed.* **2016**, 55, 6004.
- [39] V. Men Truong, J. Richard Tolchard, J. Svendby, M. Manikandan, H. A. Miller, S. Sunde, H. Yang, D. R. Dekel, O. Barnett, *Energies* **2020**, 13, 582.
- [40] B. Qin, H. Yu, J. Chi, J. Jia, X. Gao, D. Yao, B. Yi, Z. Shao, *RSC Adv.* **2017**, 7, 31574.
- [41] J. Song, C. Wei, Z. F. Huang, C. Liu, L. Zeng, X. Wang, Z. J. Xu, *Chem. Soc. Rev.* **2020**, 49, 2196.
- [42] Y. Yang, T. Yue, Y. Wang, Z. Yang, X. Jin, *Microchem. J.* **2019**, 148, 42.
- [43] T. Li, S. Li, Q. Liu, Y. Tian, Y. Zhang, G. Fu, Y. Tang, *ACS Sustain. Chem. Eng.* **2019**, 7, 17950.
- [44] E. Demir, S. Akbayrak, A. M. Onal, S. Ozkar, *J. Colloid Interface Sci.* **2019**, 534, 704.
- [45] F. Liang, Y. Yu, W. Zhou, X. Xu, Z. Zhu, *J. Mater. Chem. A* **2015**, 3, 634.
- [46] Z. Liu, N. Li, H. Zhao, Y. Zhang, Y. Huang, Z. Yin, Y. Du, *Chem. Sci.* **2017**, 8, 3211.
- [47] G. Fang, J. Cai, Z. Huang, C. Zhang, *RSC Adv.* **2019**, 9, 17891.
- [48] Q. Wu, Q. Gao, L. Sun, H. Guo, X. Tai, D. Li, L. Liu, C. Ling, X. Sun, *Chinese J. Catal.* **2021**, 42, 482.
- [49] B. Wang, P. Xi, C. Shan, H. Chen, H. Xu, K. Iqbal, W. Liu, Y. Tang, *Adv. Mater. Interfaces* **2017**, 4, 1700272.
- [50] E. Cossar, A. Oyarce Barnett, F. Seland, E. A. Baranova, *Catalysts* **2019**, 9, 814.
- [51] L. Chen, H. Jang, M. G. Kim, Q. Qin, X. Liu, J. Cho, *Inorg. Chem. Front.* **2020**, 7, 470.
- [52] G. Liu, M. Wang, Y. Wu, N. Li, F. Zhao, Q. Zhao, J. Li, *Appl. Catal., B* **2020**, 260, 118199.
- [53] Z. Sun, X. Cao, I. G. G. Martinez, M. H. Rummeli, R. Yang, *Electrochem. Commun.* **2018**, 93, 35.
- [54] B. Qiu, C. Wang, N. Zhang, L. Cai, Y. Xiong, Y. Chai, *ACS Catal.* **2019**, 9, 6484.
- [55] J. A. Haber, E. Anzenburg, J. Yano, C. Kisielowski, J. M. Gregoire, *Adv. Energy. Mater.* **2015**, 5, 1402307.
- [56] M. Favaro, W. S. Drisdell, M. A. Marcus, J. M. Gregoire, E. J. Crumlin, J. A. Haber, J. Yano, *ACS Catal.* **2017**, 7, 1248.
- [57] L. Yang, R. Liu, L. Jiao, *Adv. Funct. Mater.* **2020**, 30, 1909618.
- [58] Y. Yu, X. Peng, U. Ali, X. Liu, Y. Xing, S. Xing, *Inorg. Chem. Front.* **2019**, 6, 3255.
- [59] Y. R. Zheng, M. R. Gao, Q. Gao, H. H. Li, J. Xu, Z. Y. Wu, S. H. Yu, *Small* **2015**, 11, 182.
- [60] X. Wu, Y. Yang, T. Zhang, B. Wang, H. Xu, X. Yan, Y. Tang, *ACS Appl. Mater. Interfaces* **2019**, 11, 39841.
- [61] J.-H. Kim, K. Shin, K. Kawashima, D. H. Youn, J. Lin, T. E. Hong, Y. Liu, B. R. Wygant, J. Wang, G. Henkelman, C. B. Mullins, *ACS Catal.* **2018**, 8, 4257.
- [62] K. Obata, K. Takanebe, *Angew. Chem. Int. Ed. Engl.* **2018**, 57, 1616.
- [63] T. Zhang, X. Wu, Y. Fan, C. Shan, B. Wang, H. Xu, Y. Tang, *ChemNanoMat* **2020**, 6, 1119.
- [64] H. Sun, C. Tian, G. Fan, J. Qi, Z. Liu, Z. Yan, F. Cheng, J. Chen, C. P. Li, M. Du, *Adv. Funct. Mater.* **2020**, 30, 1910596.
- [65] W. Peng, L. Zhao, C. Zhang, Y. Yan, Y. Xian, *Electrochim. Acta* **2016**, 191, 669.

- [66] L. Sun, L. Zhou, C. Yang, Y. Yuan, *Int. J. Hydrogen Energy* **2017**, *42*, 15140.
- [67] S. Soren, I. Hota, A. K. Debnath, D. K. Aswal, K. S. K. Varadwaj, P. Parhi, *Front. Chem.* **2019**, *7*.
- [68] L. Pi, R. Jiang, W. Cai, L. Wang, Y. Wang, J. Cai, X. Mao, *ACS Appl. Mater. Interfaces* **2020**, *12*, 3642.
- [69] J. K. Norskov, J. Rossmeisl, A. Logadottir, L. Lindqvist, J. R. Kitchin, T. Bligaard, H. Jonsson, *J. Phys. Chem. B* **2004**, *108*, 17886.
- [70] V. S. Pinheiro, F. M. Souza, T. C. Gentil, P. Böhnstedt, E. C. Paz, L. S. Parreira, P. Hammer, B. L. Batista, M. C. Santos, *ChemElectroChem* **2019**, *6*, 5124.
- [71] Y. Li, X. Zhang, S. Wang, G. Sun, *ChemElectroChem* **2018**, *5*, 2442.
- [72] C. Du, X. Gao, C. Cheng, Z. Zhuang, X. Li, W. Chen, *Electrochim. Acta* **2018**, *266*, 348.
- [73] J. C. Carrillo-Rodríguez, S. García-Mayagoitia, R. Pérez-Hernández, M. T. Ochoa-Lara, F. Espinosa-Magaña, F. Fernández-Luqueño, P. Bartolo-Pérez, I. L. Alonso-Lemus, F. J. Rodríguez-Varela, *J. Power Sources* **2019**, *414*, 103.
- [74] J. C. Carrillo-Rodríguez, S. García-Mayagoitia, R. Perez-Hernandez, M. T. Ochoa-Lara, F. Espinosa-Magana, F. Fernandez-Luqeno, I. L. Alonso-Lemus, F. J. Rodriguez-Varela, *ECS Trans.*, **2017**, *77*, 1359.
- [75] J. Yang, J. Wang, L. Zhu, Q. Gao, W. Zeng, J. Wang, Y. Li, *Ceram. Int.* **2018**, *44*, 23073.
- [76] J. Yang, J. Wang, L. Zhu, W. Zeng, J. Wang, *Mater. Lett.* **2019**, *234*, 331.
- [77] X. Wang, J. Xu, Z. Wu, M. Zhi, Z. Hong, F. Huang, *ChemNanoMat* **2019**, *5*, 831.
- [78] S. Parwaiz, K. Bhunia, A. K. Das, M. M. Khan, D. Pradhan, *J. Phys. Chem. C* **2017**, *121*, 20165.
- [79] A. Sivanantham, P. Ganesan, S. Shanmugam, *Appl. Catal., B* **2018**, *237*, 1148.
- [80] Y. Yu, B. He, Y. Liao, X. Yu, Z. Mu, Y. Xing, S. Xing, *ChemElectroChem* **2018**, *5*, 793.
- [81] X. Wang, J. Xu, M. Zhi, Z. Hong, F. Huang, *J. Alloys Compd.* **2019**, *801*, 192.
- [82] M. Ji, B. He, Y. Yu, X. Yu, S. Xing, *ChemElectroChem* **2020**, *7*, 642.
- [83] Y. Kang, W. Wang, J. Li, Y. Mi, H. Gong, Z. Lei, *J. Colloid Interface Sci.* **2020**, *578*, 796.
- [84] L. Tao, Y. Shi, Y.-C. Huang, R. Chen, Y. Zhang, J. Huo, Y. Zou, G. Yu, J. Luo, C.-L. Dong, S. Yang, *Nano Energy* **2018**, *53*, 604.
- [85] L. Chen, X. Liang, X. Li, J. Pei, H. Lin, D. Jia, W. Chen, D. Wang, Y. Li, *Nano Energy* **2020**, *73*.
- [86] M. J. Paulo, R. H. D. Venancio, R. G. Freitas, E. C. Pereira, A. C. Tavares, *J. Electroanal. Chem.* **2019**, *840*, 367.
- [87] Y.-Y. Feng, H.-S. Hu, G.-H. Song, S. Si, R.-J. Liu, D.-N. Peng, D.-S. Kong, *J. Alloys Compd.* **2019**, *798*, 706.
- [88] W. Chen, J. Xue, Y. Bao, L. Feng, *Chem. Eng. J.* **2020**, *381*, 122752.
- [89] M. Sedighi, A. A. Rostami, E. Alizadeh, *Int. J. Hydrogen Energy* **2017**, *42*, 4998.
- [90] H. Xu, A.-L. Wang, Y.-X. Tong, G.-R. Li, *ACS Catal.* **2016**, *6*, 5198.
- [91] H. Wang, Y. Xue, B. Zhu, J. Yang, L. Wang, X. Tan, Z. Wang, Y. Chu, *Int. J. Hydrogen Energy* **2017**, *42*, 20549.
- [92] F. Xie, L. Ma, M. Gan, H. He, L. Hu, M. Jiang, H. Zhang, *Appl. Surf. Sci.* **2019**, *481*, 1425.
- [93] Y. Zheng, X. Zhang, Z. Zhang, Y. Li, Y. Sun, Y. Lou, X. Li, Y. Lu, *J. Rare Earths* **2018**, *36*, 974.
- [94] D. V. Dao, T. D. Le, G. Adilbish, I.-H. Lee, Y.-T. Yu, *J. Mater. Chem. A* **2019**, *7*, 26996.
- [95] T. Gentil, V. Pinheiro, E. Paz, F. Souza, L. Parreira, M. Santos, *J. Brazil. Chem. Soc.* **2019**.
- [96] Y. Zheng, Z. Zhang, X. Zhang, H. Ni, Y. Sun, Y. Lou, X. Li, Y. Lu, *Mater. Lett.* **2018**, *221*, 301.
- [97] C. Liu, L. Zhang, L. Sun, W. Wang, Z. Chen, *Int. J. Hydrogen Energy* **2020**, *45*, 8558.
- [98] D. Chai, W. Wang, F. Wang, W. Jing, P. Wang, Z. Lei, *Int. J. Hydrogen Energy* **2017**, *42*, 9775.
- [99] W. Li, Z. Song, X. Deng, X.-Z. Fu, J.-L. Luo, *Electrochim. Acta* **2020**, *337*.
- [100] P. Salarizadeh, M. B. Askari, M. Mohammadi, K. Hooshyari, *J. Phys. Chem. Solids* **2020**, *142*, 109442.
- [101] G. Valenti, M. Melchionna, T. Montini, A. Boni, L. Nasi, E. Fonda, A. Criado, A. Zitolo, S. Voci, G. Bertoni, M. Bonchio, P. Fornasiero, F. Paolucci, M. Prato, *ACS Appl. Energy Mater.* **2020**, *3*, 8509, <https://doi.org/10.1002/acs.202002133>.
- [102] J. Fu, D. Ren, M. Xiao, K. Wang, Y. Deng, D. Luo, J. Zhu, G. Wen, Y. Zheng, Z. Bai, L. Yang, Z. Chen, *ChemSusChem* **2020**.
- [103] S. B. Varandili, J. Huang, E. Oveisi, G. L. De Gregorio, M. Mensi, M. Strach, J. Vavra, C. Gadiyar, A. Bhowmik, R. Buonsanti, *ACS Catal.* **2019**, *9*, 5035.
- [104] D. Wu, C. Dong, D. Wu, J. Fu, H. Liu, S. Hu, Z. Jiang, S. Z. Qiao, X.-W. Du, *J. Mater. Chem. A* **2018**, *6*, 9373.
- [105] Q. Zhang, J. Du, A. B. He, Z. H. Liu, C. Y. Tao, *J. Solid State Chem.* **2019**, *279*, 9.
- [106] B. Xu, L. Xia, F. Zhou, R. Zhao, H. Chen, T. Wang, Q. Zhou, Q. Liu, G. Cui, X. Xiong, F. Gong, X. Sun, *ACS Sustain. Chem. Eng.* **2019**, *7*, 2889.
- [107] H. Xie, Q. Geng, X. Li, T. Wang, Y. Luo, A. A. Alshehri, K. A. Alzahrani, B. Li, Z. Wang, J. Mao, *Chem Commun.* **2019**, *55*, 10717.
- [108] S. Zhang, C. Zhao, Y. Liu, W. Li, J. Wang, G. Wang, Y. Zhang, H. Zhang, H. Zhao, *Chem Commun.* **2019**, *55*, 2952.
- [109] H. Xie, H. Wang, Q. Geng, Z. Xing, W. Wang, J. Chen, L. Ji, L. Chang, Z. Wang, J. Mao, *Inorg. Chem.* **2019**, *58*, 5423.
- [110] S. J. Li, D. Bao, M. M. Shi, B. R. Wulan, J. M. Yan, Q. Jiang, *Adv. Mater.* **2017**, *29*, 1606550.
- [111] C. Lv, C. Yan, G. Chen, Y. Ding, J. Sun, Y. Zhou, G. Yu, *Angew. Chem. Int. Ed.* **2018**, *57*, 6073.
- [112] J. Qi, L. Gao, F. Wei, Q. Wan, S. Lin, *ACS Appl. Mater. Interfaces* **2019**, *11*, 47525.
- [113] N. R. Manwar, A. A. Chilkalwar, K. K. Nanda, Y. S. Chaudhary, J. Subrt, S. S. Rayalu, N. K. Labhsetwar, *ACS Sustain. Chem. Eng.* **2016**, *4*, 2323.
- [114] Z. Cheng, F. Wang, T. A. Shifa, C. Jiang, Q. Liu, J. He, *Small* **2017**, *13*, 1702163.
- [115] B. Dong, L. Li, Z. Dong, R. Xu, Y. Wu, *Int. J. Hydrogen Energy* **2018**, *43*, 5275.
- [116] A. Krishnan, S. Beena, M. Chandran, *Mater. Today: Proc.* **2019**, *18*, 4968.
- [117] N.-C. Zheng, T. Ouyang, Y. Chen, Z. Wang, D.-Y. Chen, Z.-Q. Liu, *Catal. Sci. Technol.* **2019**, *9*, 1357.
- [118] Y. Ma, Y. Bian, Y. Liu, A. Zhu, H. Wu, H. Cui, D. Chu, J. Pan, *ACS Sustain. Chem. Eng.* **2018**, *6*, 2552.
- [119] S. Sultana, S. Mansingh, M. Scurrell, K. M. Parida, *Inorg. Chem.* **2017**, *56*, 12297.
- [120] J. Qian, Z. Chen, H. Sun, F. Chen, X. Xu, Z. Wu, P. Li, W. Ge, *ACS Sustain. Chem. Eng.* **2018**, *6*, 9691.
- [121] J. Qian, Z. Chen, F. Chen, Y. Wang, Z. Wu, W. Zhang, Z. Wu, P. Li, *Inorg. Chem.* **2018**, *57*, 14532.
- [122] G. Swain, S. Sultana, B. Naik, K. Parida, *ACS Omega* **2017**, *2*, 3745.
- [123] M. Sridharan, P. Kamaraj, Y. S. Huh, S. Devikala, M. Arthanareeswari, J. A. Selvi, E. Sundaravadivel, *Catal. Sci. Technol.* **2019**, *9*, 3686.
- [124] Y. Wang, X. Hao, L. Zhang, Y. Li, Z. Jin, *Energy Fuels* **2020**, *34*, 2599.
- [125] X. Cui, Z. Liu, G. Li, M. Zhang, Y. Song, J. Wang, *Int. J. Hydrogen Energy* **2019**, *44*, 23921.
- [126] X. Liu, L. He, X. Chen, L. Du, X. Gu, S. Wang, M. Fu, F. Dong, H. Huang, *Int. J. Hydrogen Energy* **2019**, *44*, 16154.
- [127] M. Waqas, B. Yang, L. Cao, X. Zhao, W. Iqbal, K. Xiao, C. Zhu, J. Zhang, *Catal. Sci. Technol.* **2019**, *9*, 5322.

- [128] C. Zhu, Y. Wang, Z. Jiang, F. Xu, Q. Xian, C. Sun, Q. Tong, W. Zou, X. Duan, S. Wang, *Appl. Catal., B* **2019**, 259, 118072.
- [129] H. Yu, J. Xu, C. Yin, Z. Liu, Y. Li, *J. Solid State Chem.* **2019**, 272, 102.
- [130] M. Li, L. Zhang, M. Wu, Y. Du, X. Fan, M. Wang, L. Zhang, Q. Kong, J. Shi, *Nano Energy* **2016**, 19, 145.
- [131] Z. Han, Y. Yu, W. Zheng, Y. Cao, *New J. Chem.* **2017**, 41, 9724.
- [132] M. Liang, T. Borjigin, Y. Zhang, B. Liu, H. Liu, H. Guo, *Appl. Catal. B* **2019**, 243, 566.
- [133] M. Wang, M. Shen, X. Jin, J. Tian, M. Li, Y. Zhou, L. Zhang, Y. Li, J. Shi, *ACS Catal.* **2019**, 9, 4573.
- [134] H. Wang, J. Guan, J. Li, X. Li, C. Ma, P. Huo, Y. Yan, *Appl. Surf. Sci.* **2020**, 506, 144931.
- [135] P. Seeharaj, P. Kongmun, P. Paipod, S. Prakobmit, C. Sriwong, P. Kim-Lohsoontorn, N. Vittayakorn, *Ultrason. Sonochem.* **2019**, 58, 104657.
- [136] J. Zheng, Z. Zhu, G. Gao, Z. Liu, Q. Wang, Y. Yan, *Catal. Sci. Technol.* **2019**, 9, 3788.
- [137] J. Guan, H. Wang, J. Li, C. Ma, P. Huo, *J. Taiwan. Inst. Chem. E.* **2019**, 99, 93.
- [138] Y. Wang, X. Bai, F. Wang, S. Kang, C. Yin, X. Li, *J. Hazard. Mater.* **2019**, 372, 69.
- [139] B. Huang, R. Gillen, J. Robertson, *J. Phys. Chem. C* **2014**, 118, 24248.
- [140] X. Cai, K. Chen, X. Gao, C. Xu, M. Sun, G. Liu, X. Guo, Y. Cai, B. Huang, J. Deng, J. Z. Liu, A. Tricoli, N. Wang, C. Dwyer, Y. Zhu, *Chem. Mater.* **2019**, 31, 5769.
- [141] J. Xia, H. Zhao, B. Huang, L. Xu, M. Luo, J. Wang, F. Luo, Y. Du, C. H. Yan, *Adv. Funct. Mater.* **2020**, 30, 1908367.
- [142] S. Bai, F. Liu, B. Huang, F. Li, H. Lin, T. Wu, M. Sun, J. Wu, Q. Shao, Y. Xu, X. Huang, *Nat Commun* **2020**, 11, 954.
- [143] D. Tian, K. Li, Y. Wei, X. Zhu, C. Zeng, X. Cheng, Y. Zheng, H. Wang, *Phys. Chem. Chem. Phys.* **2018**, 20, 11912.
- [144] R. Bose, K. Karuppasamy, H. Rajan, D. B. Velusamy, H.-S. Kim, A. Alfantazi, *ACS Sustain. Chem. Eng.* **2019**, 7, 16392.



Qingqing Li received his B.S. degree from Taiyuan University of Technology in 2016 and his M.S. in chemical engineering from Guangzhou Institute of Energy Conversion, Chinese Academy of Science. Then, he joined Prof. Feng Luo and Prof. Yaping Du's group as a Ph.D. candidate. He currently works on rare-earth based electrocatalysis.



Bolong Huang received Ph.D. in 2012 from University of Cambridge, and he obtained B.Sc. from Peking University in 2007. Following a systematic training period as research assistant in Peking University and Hong Kong, he is now an assistant Professor in the Hong Kong Polytechnic University. His main research fields are DFT calculations on rare earth functional nanomaterials, defect theory of solid functional nanomaterials, DFT calculation development based on ab initio electronic self-energy corrections, and semicore orbital corrections as an implement in time-dependent DFT theory.



Yaping Du is a full professor at the School of Materials Science and Engineering, Nankai University and the director of Tianjin Key Lab for Rare Earth Materials and Applications. His research interests focus on rare-earth functional materials, and colloidal inorganic nanocrystals, and energy storage and conversion materials. In 2004, he received his B.S. degree from Lanzhou University, and in 2009, he received his Ph.D. degree from Peking University.



Chun-Hua Yan received his Ph.D. from Peking University at 1988. He was elected as a Member of the Chinese Academy of Sciences in 2011, and a Fellow of the Academy of Sciences for the Developing World (TWAS) in 2012. He is the president of Lanzhou University and the director of the State Key Laboratory of Rare Earth Materials Chemistry and Applications at Peking University, and the Centre for Rare Earth and Inorganic Functional Materials at Nankai University.